Lecture: Active remote sensing of the Atmosphere

Dual-Field-of-View Lidar: a tool for assessing liquid-cloud microphysics

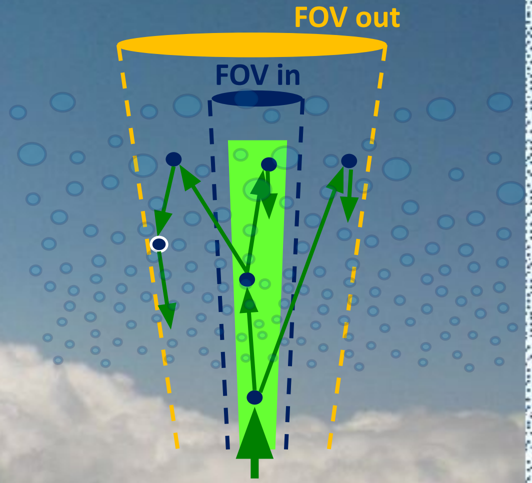

J. Bühl for: C. Jimenez (jimenez@tropos.de), A. Ansmann, R. Engelmann, P. Seifert, U. Wandinger, H. Baars and the remote-sensing team of TROPOS.

1. **Aerosol, clouds and lidar.**
2. **Lidar multiple-scattering, dual-field-of-view and cloud-retrieval techniques**
3. **Application and potential research.**

TROPOS

8 January 2025

- Clouds are a big component in Earth‘s atmosphere.
- Their formation and evolution are governed by meteorological conditions (**aerosol, water vapor, vertical wind**)
- There are **multiple processes** shaping cloud macro- and microphysics and thermodynamics.

Introduction: aerosol-cloud interactions

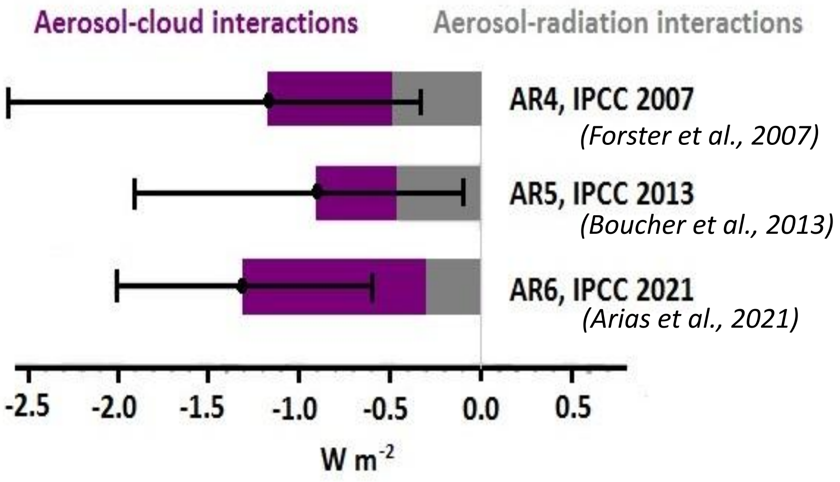

Warm clouds

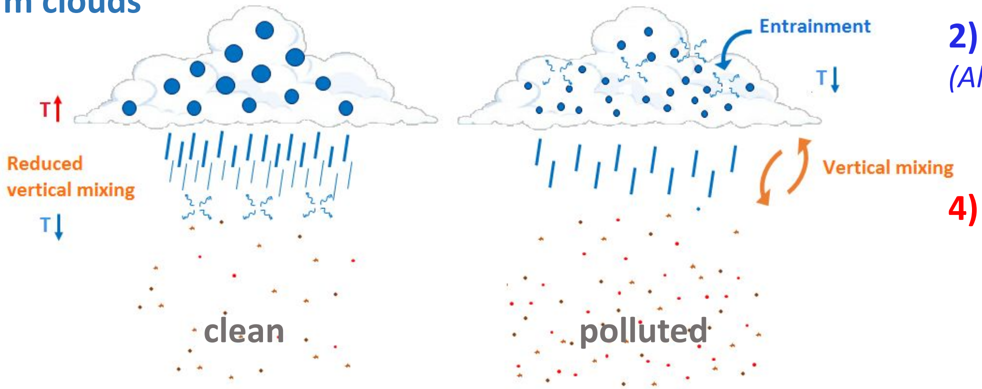

2) Drizzle suppression
(Albrecht, 1989, Rosenfeld, 1999)

3) Enhanced mixing at CB
(Albrecht, 1989)

4) Faster evaporation
(Ackermann et al., 2004)

5) More entrainment
(Ackermann et al., 2004)

Convective and cold clouds

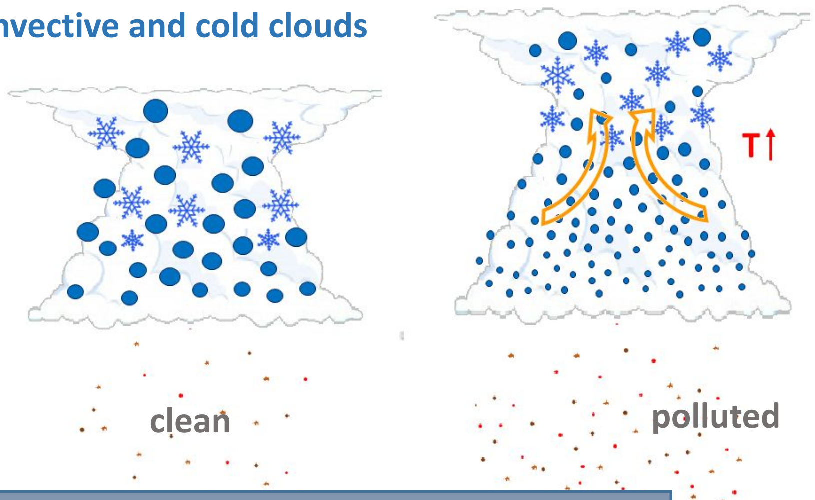

6) Combined INP-CCN Twomey effect
(MPC, Lohmann, 2017, Maciel et al., 2023)

7) Freezing starts higher
(Lohmann, 2016)

8) Updrafts invigorated
(Koren et al., 2005, Zang et al., 2023)

9) WBF process
(Wegener, 1911; Bergeron, 1935; Findeisen, 1938)

Total radiative effect

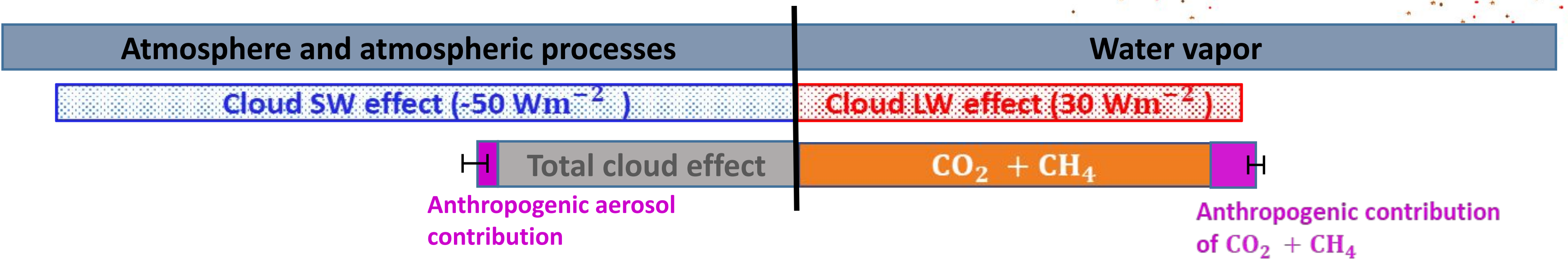

Cloud processes vs Aerosol-cloud interactions

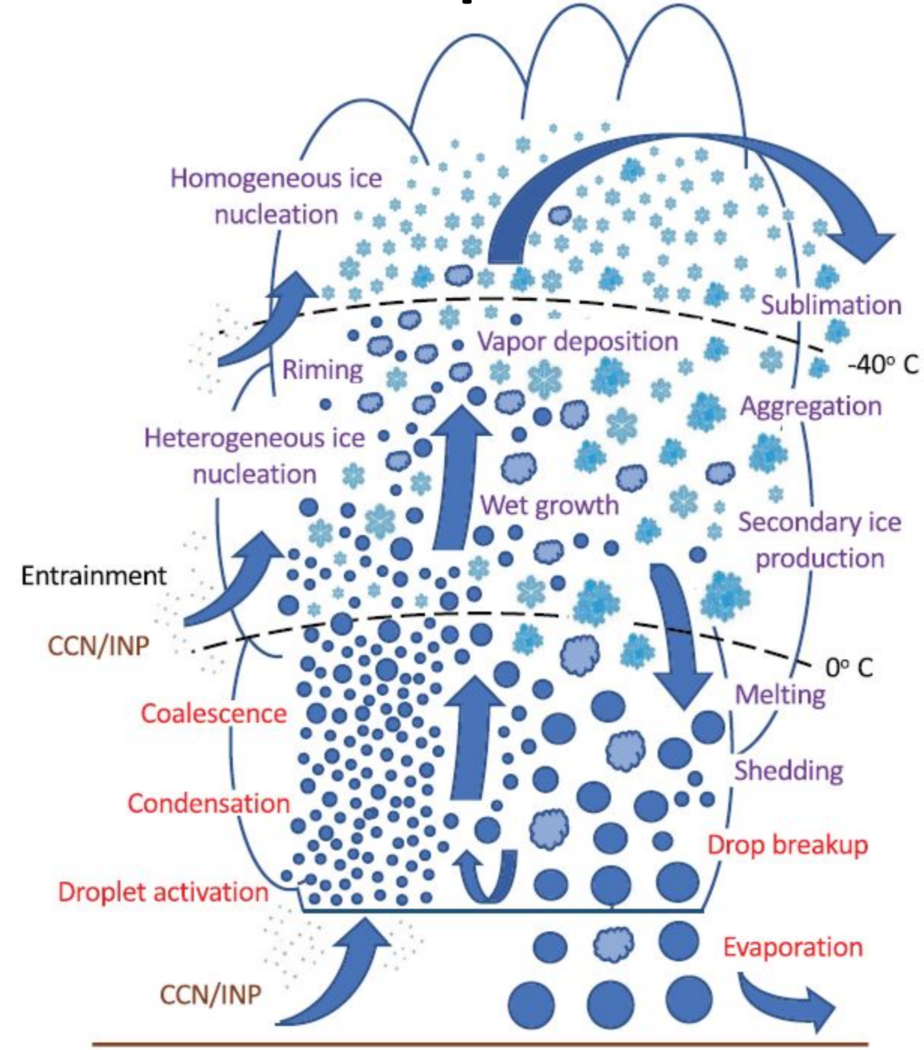

(Morrison et al. 2020)

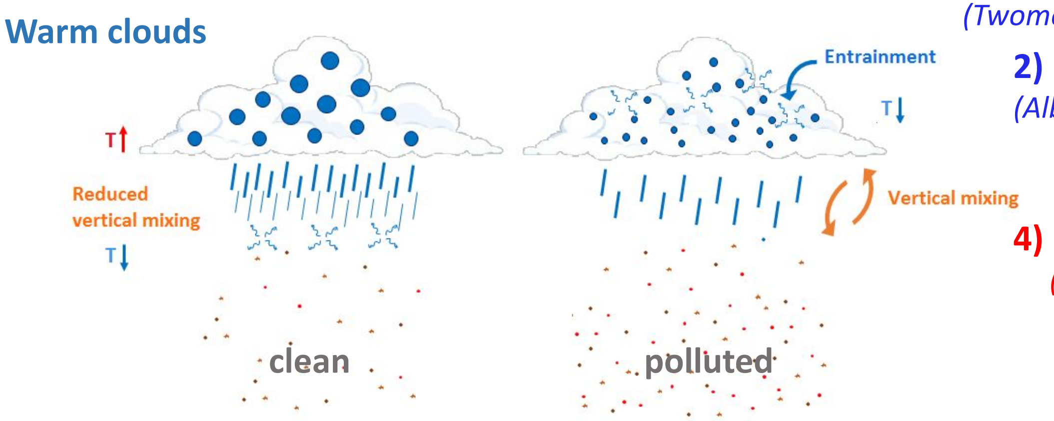

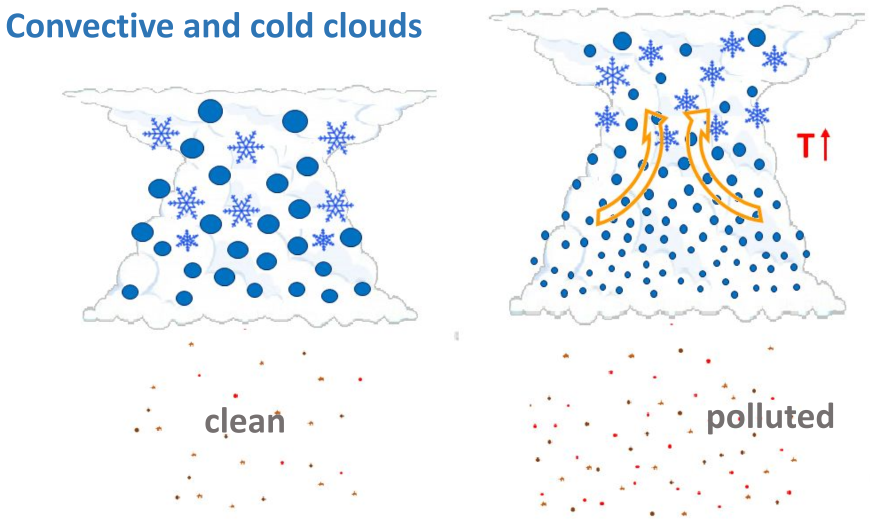

1) Increase cloud albedo
(Twomey, 1959)

2) Drizzle suppression
(Albrecht, 1989, Rosenfeld, 1999)

3) Enhanced mixing at CB
(Albrecht, 1989)

4) Faster evaporation
(Ackermann et al., 2004)

5) More entrainment
(Ackermann et al., 2004)

6) Combined INP-CCN Twomey effect
(MPC, Lohmann, 2017, Maciel et al., 2023)

7) Freezing starts higher
(Lohmann, 2016)

8) Updrafts invigorated
(Koren et al., 2005, Zang et al., 2023)

9) WBF process
(Wegener, 1911; Bergeron, 1935; Findeisen, 1938)

We need observations of aerosol and cloud microphysics

Ice-nuclei / ice-crystal life cycle

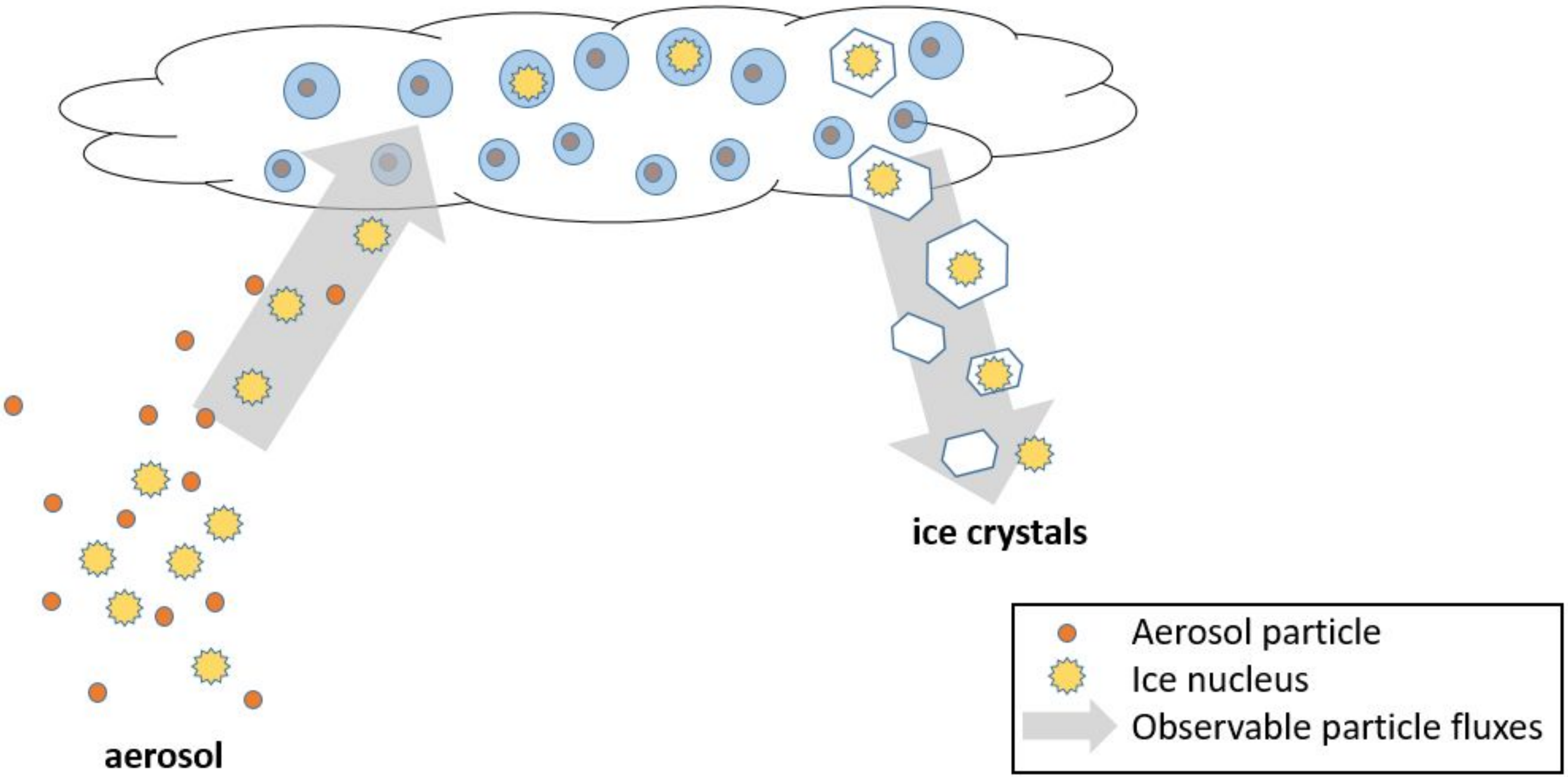

Overview of analysis flow at TROPOS

Lidar signals

- 355 (elastic, II, ⊥)
- 387 (Raman, N_2)
- 407 (Raman, H_2O)
- 466 (Fluoresc.)
- 532(elastic, II, ⊥)
- 607 ((Raman, N_2)
- 1064 (elastic)

…

- **Dual-FOV measurements**
- Rotational Raman measurements
- HSRL (Mie - Rayleigh)
- DIAL
- Doppler shift

Calibrations and usage of external information (P(z), T(z), RH(z))

Lidar products

Extensive properties (dependent of number concentration):

- Extinction: $\alpha_{355}, \alpha_{532}$
- Backscatter: $\beta_{355}, \beta_{532}, \beta_{1064}$
- Fluorescence backscatter: β_{466}
- Volume depolarization ratio: $\delta_{355}, \delta_{532}$

Intensive properties (independent of concentration):

- Lidar ratio: LR_{355}, LR_{532}
- Ångström exp: $Å_{355/532}$, $Å_{\beta355/\beta1064}$, $Å_{\beta532/\beta1064}$
- Particle depol: $\delta^p_{355}, \delta^p_{532}$
- Fluoresc. Capacity: $F_{C,466}$

Typing &/or size information

Microphysical properties of aerosol particles

Overview of analysis flow at TROPOS

Lidar signals

- 355 (elastic, II, ⊥)
- 387 (Raman, N_2)
- 407 (Raman, H_2O)
- 466 (Fluoresc.)
- 532(elastic, II, ⊥)
- 607 ((Raman, N_2)
- 1064 (elastic)

…

- **Dual-FOV measurements**
- Rotational Raman measurements
- HSRL (Mie - Rayleight)
- DIAL
- Doppler shift

Calibrations and usage of external information (P(z), T(z), RH(z))

Lidar products

Extensive properties (dependent of number concentration):

- Extinction: $\alpha_{355}, \alpha_{532}$
- Backscatter: $\beta_{355}, \beta_{532}, \beta_{1064}$
- Fluorescence backscatter: β_{466}
- Volume depolarization ratio: $\delta_{355}, \delta_{532}$

Intensive properties (independent of concentration):

- Lidar ratio: LR_{355}, LR_{532}
- Ångström exp: $Å_{355/532}$, $Å_{\beta355/\beta1064}$, $Å_{\beta532/\beta1064}$
- Particle depol: $\delta^p_{355}, \delta^p_{532}$
- Fluoresc. Capacity: $F_{C,466}$

Typing &/or size information

Microphysical properties of aerosol particles

Microphysical properties of clouds

Cloud relevant products: $CCNC, INPC, CDNC, ICNC$

Some insights into particle microphysics

- $P(z) = \frac{O(z)}{z^2} C_l \beta_{\lambda_0}(z) T^2_{\lambda_0}(z)$

Particle extinction coefficient $\alpha_{\lambda_0,\mathrm{par}} = \int n(r)\sigma_{\lambda_0,ext}(r)\mathrm{d}r = \int n(r)\pi r^2 Q_{\lambda_0,ext}(r)\mathrm{d}r$

extinction efficiency

extinction cross section

Geometrical cross section

Depends on size and number density!

Type □ constrain a size distribution and efficiency

Poliphon (*Mamouri & Ansmann 2016),*

Inversion (*Veselovskii et al 2002*)

Particle number concentration N_{par}

What happens in liquid-water clouds?

- Efficiency is known $Q_{\lambda_0,ext}(r) \approx 2$
- Unknown size distribution $n(r)$
- **Lidar equation breaks because of multiple scattering**

Single scattering

$$T_{\lambda_0}(z) = \exp\left\{-\int_0^z \left[\alpha_{\lambda_0,\mathrm{par}}(\xi) + \alpha_{\lambda_0,\mathrm{mol}}(\xi)\right] d\xi\right\}$$

Multiple scattering

$$T_{\lambda_0}(z) = \exp\left\{-\int_0^z \left[(1-\boldsymbol{F_{MS}})\alpha_{\lambda_0,\mathrm{par}}(\xi) + \alpha_{\lambda_0,\mathrm{mol}}(\xi)\right] d\xi\right\}$$

A third unknown emerges in the lidar equation. The multiple scattering fraction F_{MS}

Light scattering at particles

Scattering phase function

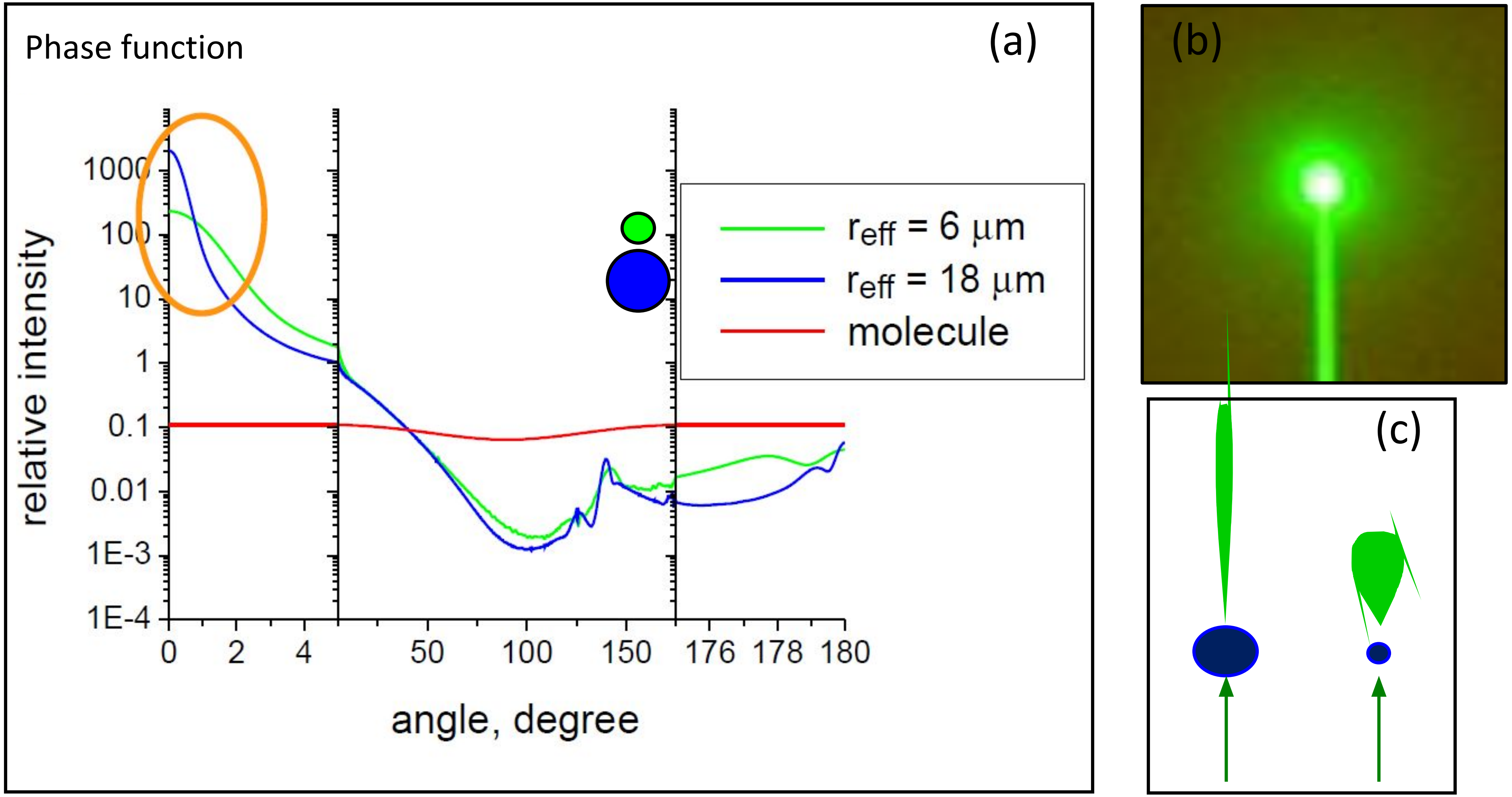

PollyXT Lidar aboard FS Polarstern (MOSAIC campaign)

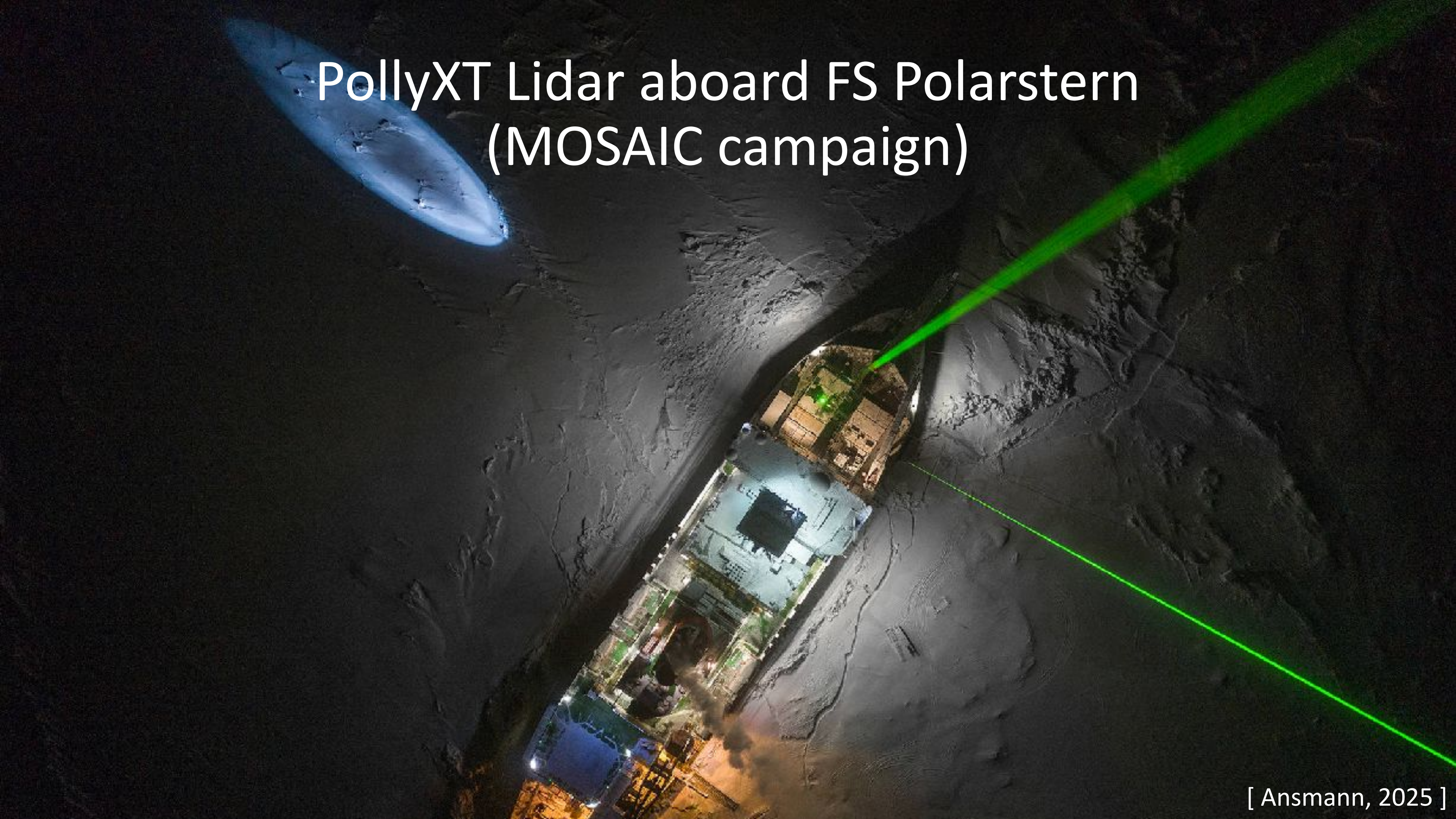

[Ansmann, 2025]

[Ansmann, 2025]

Some insights into multiple scattering

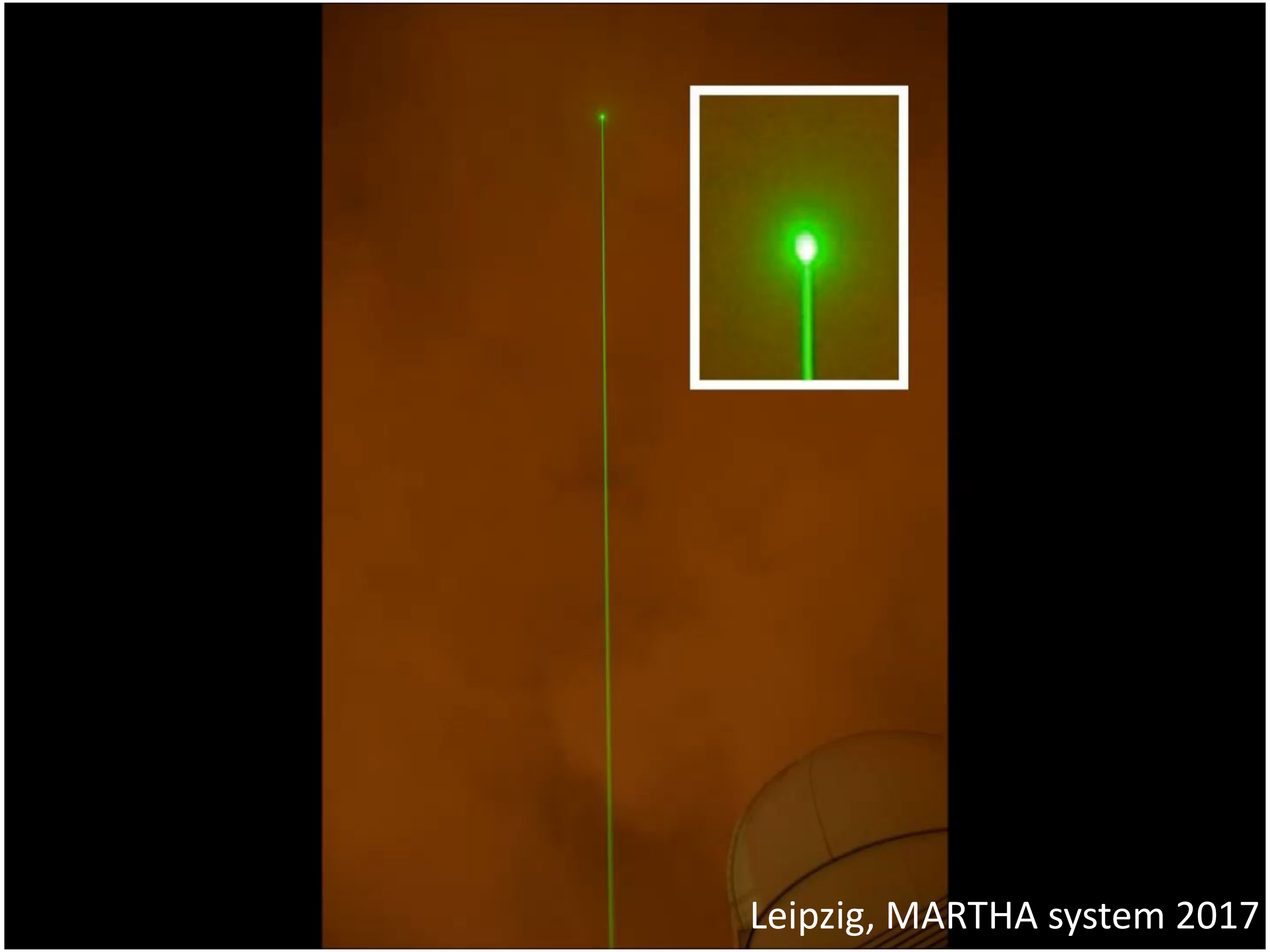

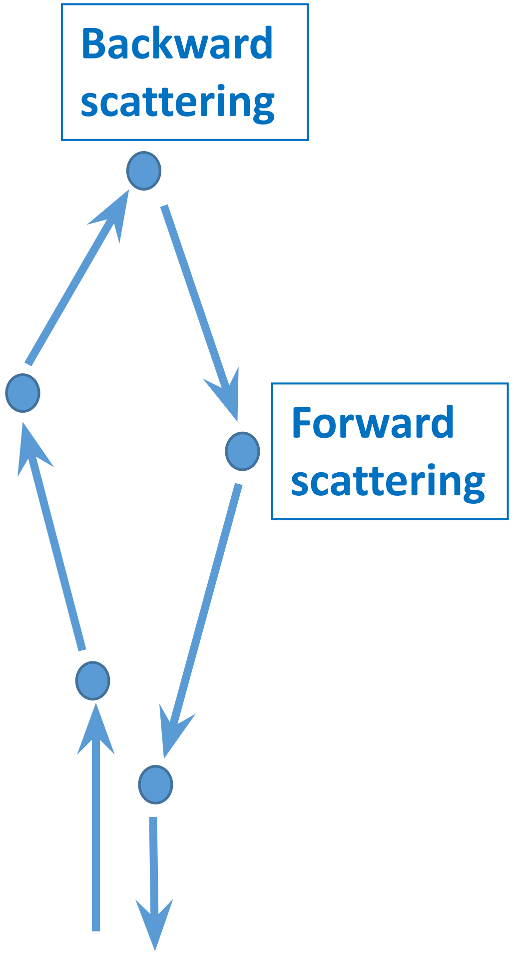

Some insights into multiple scattering

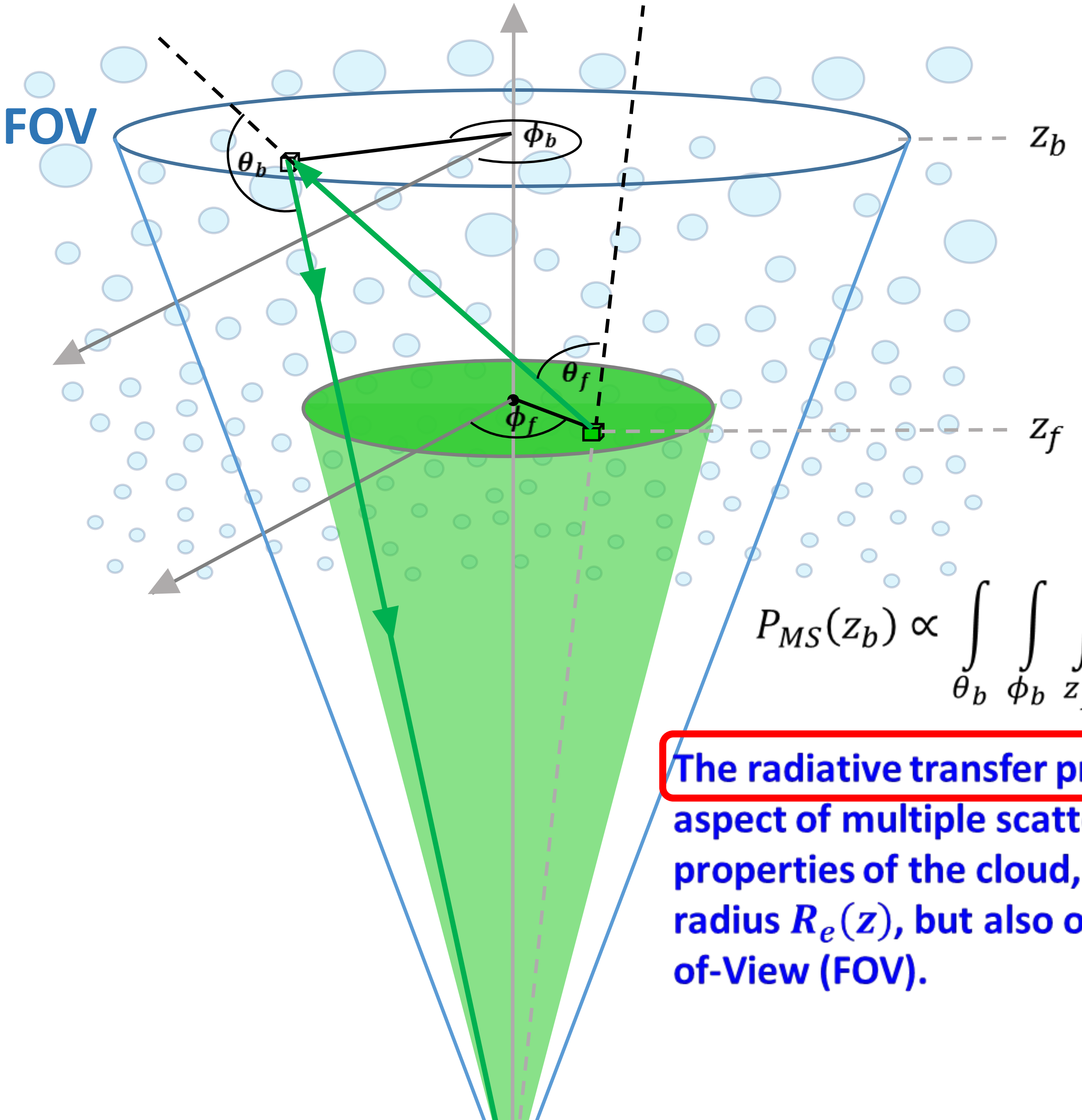

Example of
double scattering

Multiple scattering fraction:

$$F_{MS} = \frac{P_{MS}}{P_{MS} + P_{SS}}$$

P_{SS}: Single-scattering lidar return
P_{MS}: Multiple-scattering lidar return

$$P_{MS}(z_b) \propto \int_{\theta_b} \int_{\phi_b} \int_{z_f} \int_{\theta_f} \int_{\phi_f} I_{very-difficult}(z_f, \theta_f, \phi_f, z_b, \theta_b, \phi_b, \alpha(z), R_e(z), \theta_{FOV})$$

The radiative transfer problem is difficult to solve. The favorable aspect of multiple scattering is that it depends on the microphysical properties of the cloud, the extinction coefficient $\alpha(z)$ and effective radius $R_e(z)$, but also on lidar geometry, namely the receiver Field-of-View (FOV).

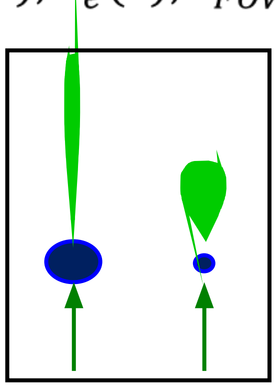

Modeling of lidar multiple scattering

$$\boldsymbol{S_i^{(2)}}(z_\mathrm{b}) = \int_0^{\psi_\mathrm{FOV}} \theta_\mathrm{b} d\theta_\mathrm{b} \int_0^{2\pi} d\phi_\mathrm{b} \int_{z_\mathrm{CB}}^{z_\mathrm{b}} dz_\mathrm{f} \int_0^{\theta_\mathrm{max}} \theta_\mathrm{f} d\theta_\mathrm{f} \int_0^{2\pi} \frac{\alpha(z_\mathrm{f})\alpha(z_\mathrm{b})}{(z_\mathrm{b}-z_\mathrm{f})^2} I_L(\theta_\mathrm{f},\phi_\mathrm{f})\ S_i^{(2)\,\mathrm{f}\to\mathrm{b}} d\phi_\mathrm{f}$$

+

$$\int_0^{\theta_\mathrm{max}} \theta_\mathrm{b} d\theta_\mathrm{b} \int_0^{2\pi} d\phi_\mathrm{b} \int_{z_\mathrm{CB}}^{z_\mathrm{b}} dz_\mathrm{f} \int_0^{\psi_\mathrm{FOV}} \theta_\mathrm{f} d\theta_\mathrm{f} \int_0^{2\pi} \frac{\alpha(z_\mathrm{b})\alpha(z_\mathrm{f})}{(z_\mathrm{b}-z_\mathrm{f})^2} I_L(\theta_\mathrm{f},\phi_\mathrm{f})\ S_i^{(2)\,\mathrm{b}\to\mathrm{f}} d\phi_\mathrm{f}$$

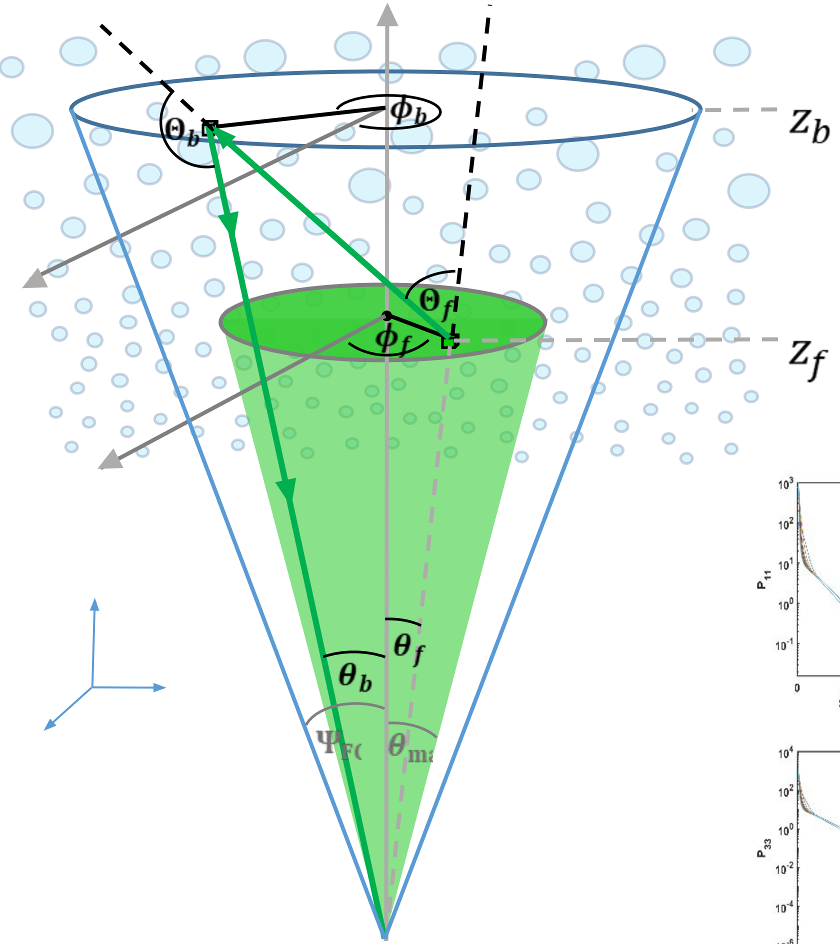

Where

$$S_i^{(2)\,\mathrm{f}\to\mathrm{b}} = S_i^{(2)\,\mathrm{f}\to\mathrm{b}}(z_\mathrm{f},\theta_\mathrm{f},\phi_\mathrm{f},z_\mathrm{b},\theta_\mathrm{b},\phi_\mathrm{b},M_\mathrm{scat}(R_\mathrm{e},\Theta_\mathrm{f},\Theta_\mathrm{b}))$$

First forward then backward

$$S_i^{(2)\,\mathrm{b}\to\mathrm{f}} = S_i^{(2)\,\mathrm{b}\to\mathrm{f}}(z_\mathrm{b},\theta_\mathrm{b},\phi_\mathrm{b},z_\mathrm{f},\theta_\mathrm{f},\phi_\mathrm{f},M_\mathrm{scat}(R_\mathrm{e},\Theta_\mathrm{b},\Theta_\mathrm{f}))$$

First backward then forward

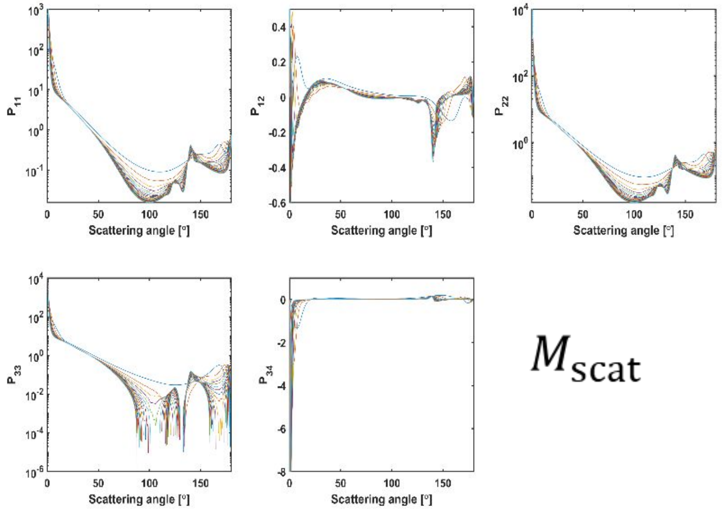

Modified Shipley model (Wandinger PhD thesis, 1994)

M_scat

Multiple scattering to assess liquid-cloud microphysics

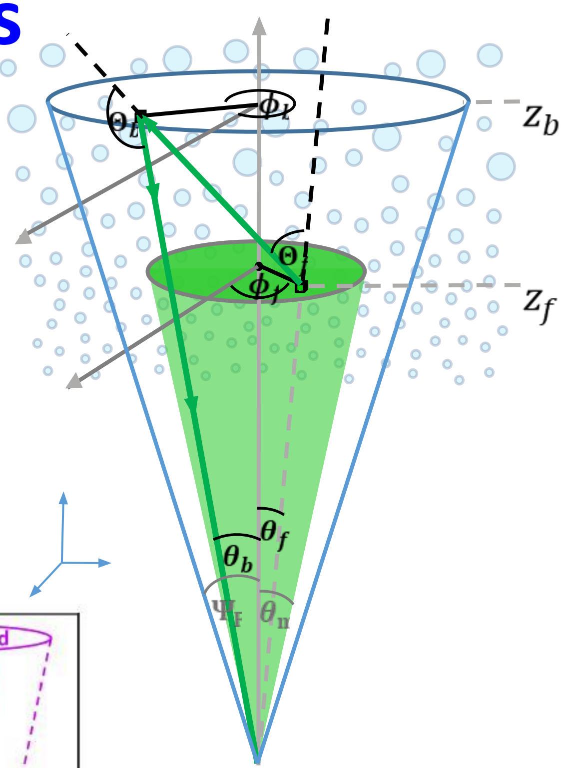

There are different approaches to solve lidar multiple scattering problem (since the 1970s):

- Monte Carlo, Stochastic methods, **semi-analytical methods.**

Methods have been proposed to use multiple scattering to retrieve cloud microphysical properties, most of them based on Dual-FOV lidars.

- Multiple FOV lidar (since 1990s).
- Dual-FOV Raman lidar (at TROPOS since 2010).
- Dual-FOV polarization lidar (at TROPOS since 2017).
- Dual-FOV high-spectral-resolution lidar (since 2020s).

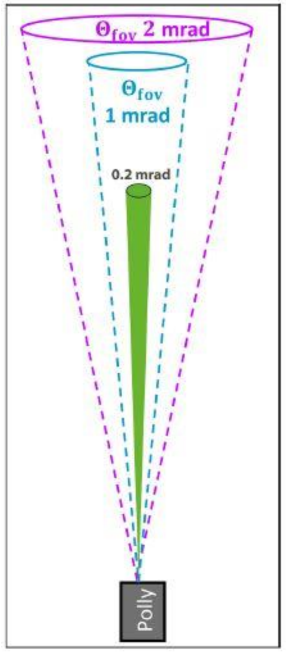

1. Dual-FOV Raman lidar

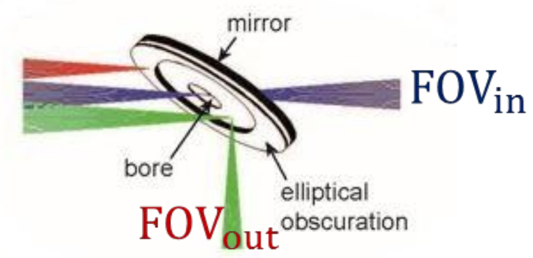

ACI studies 2010-2015 at TROPOS, *Schmidt et al., 2013, 2014, 2015.*

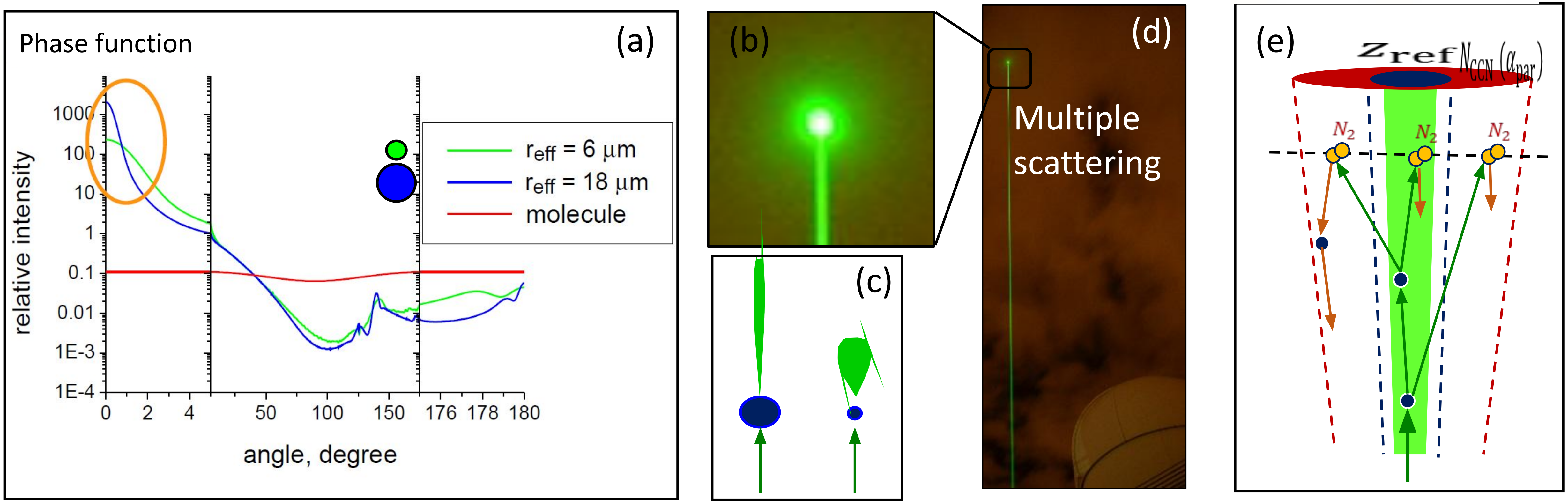

- **Multiple-scattering problem is much more simple Fast multiple-scattering model *(Malinka and Zege, 2003)***
- **Iterative procedure. No assumptions about the vertical structure.**
- **Needs large averaging periods (15-30 minutes) and works only during nighttime!**

Microphysical relations

$Q_{\lambda_0,ext}(r) \approx 2$

N_d: Droplet number concentration $\int n(r)\mathrm{d}r$

R_S^2: surface mean radius $\int n(r)r^2\mathrm{d}r \big/ \int n(r)\mathrm{d}r$

R_V^3: volume mean radius $\int n(r)r^3\mathrm{d}r \big/ \int n(r)\mathrm{d}r$

Extinction coefficient

$$\alpha = \int n(r)\pi r^2 Q_{\lambda_0,ext}(r)\mathrm{d}r = 2\pi \int n(r)r^2\mathrm{d}r = \boldsymbol{2\pi R_s^2 N_d}$$

Liquid water content

$$w_l = \frac{4}{3}\pi\rho_w \int n(r)r^3\mathrm{d}r = \frac{4}{3}\pi\rho_w \left(\frac{\int n(r)r^3\mathrm{d}r}{\int n(r)\mathrm{d}r}\right)\int n(r)\mathrm{d}r = \boldsymbol{\frac{4}{3}\pi\rho_w R_V^3 N_d = \frac{2}{3}\rho_w \alpha R_e}$$

Effective radius

$$R_e = \frac{\int n(r)r^3\mathrm{d}r}{\int n(r)r^2\mathrm{d}r} = \frac{N_d R_V^3}{N_d R_S^2} \Rightarrow \boldsymbol{R_S^2 = \frac{R_V^3}{R_e} = kR_e^2}$$

There is a linear relationship between R_V^3 and R_e^3 (*Martin et al., 1994*).

$$\boldsymbol{k = \frac{R_V^3}{R_e^3}}$$

The value of ***k*** is related to the width of the size distribution

Droplet number concentration

$$\boldsymbol{N_d = \frac{1}{2\pi k}\alpha R_e^{-2}}$$

From the extinction coefficient α and effective radius R_e, we can derive the liquid water content w_l and droplet number concentration N_d

1. Dual-FOV Raman lidar - example

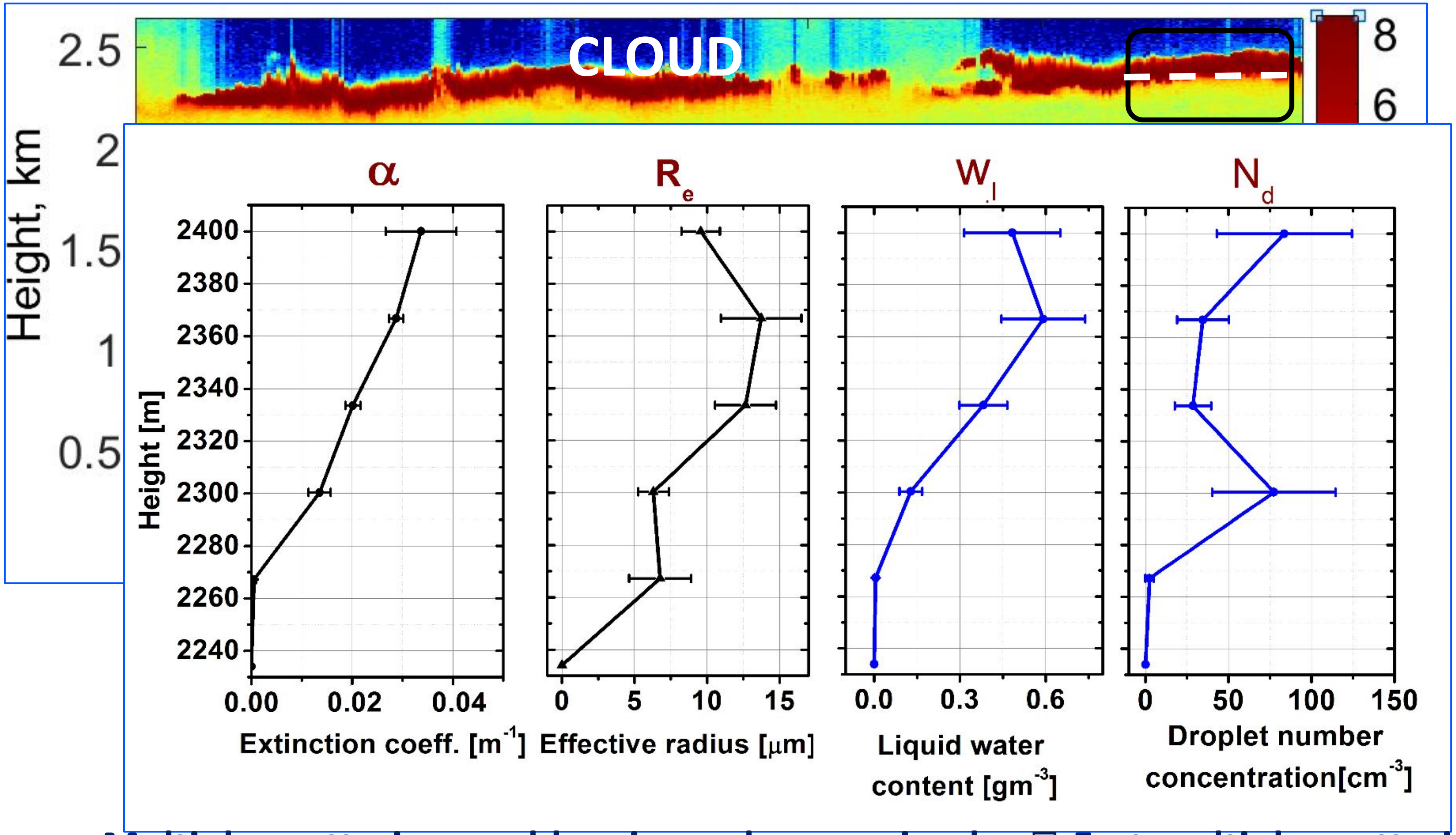

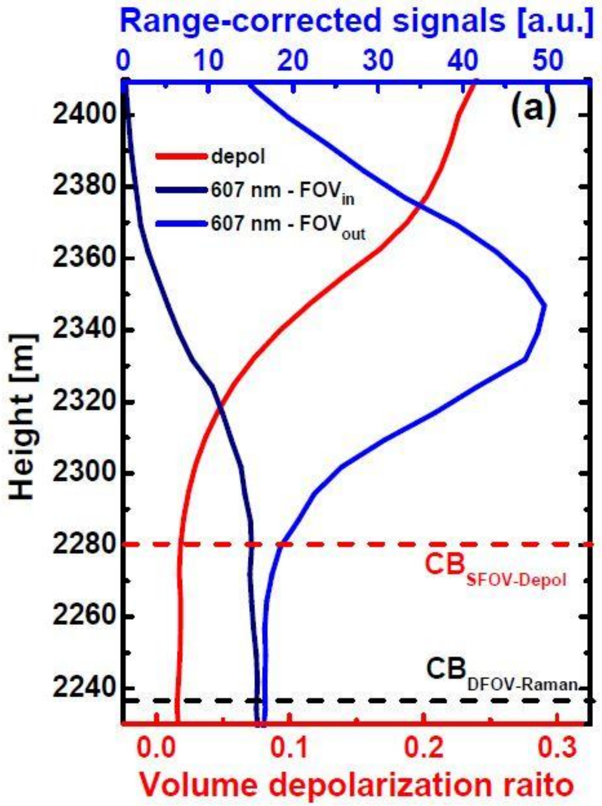

- Multiple-scattering problem is much more simpler Fast multiple-scattering model *(Malinka and Zege, 2003)*.
- Iterative procedure. No assumptions about the vertical structure.
- **Needs large averaging periods (15-30 minutes) and works only during nighttime!**

2. Dual-FOV high-spectral-resolution lidar (DFOV-HSRL)

(Wang et al., 2022)

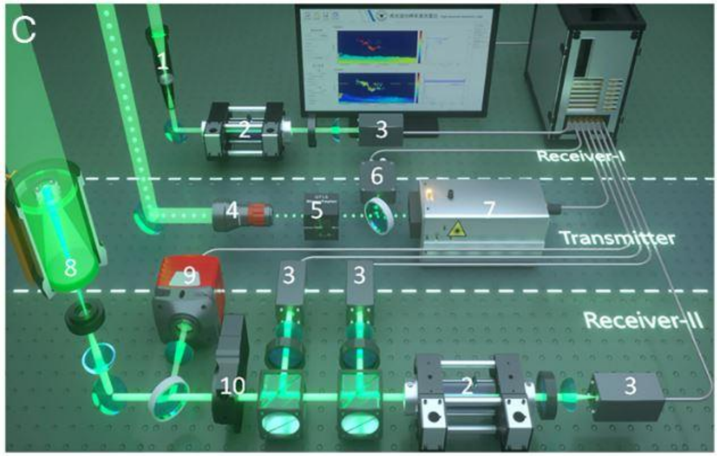

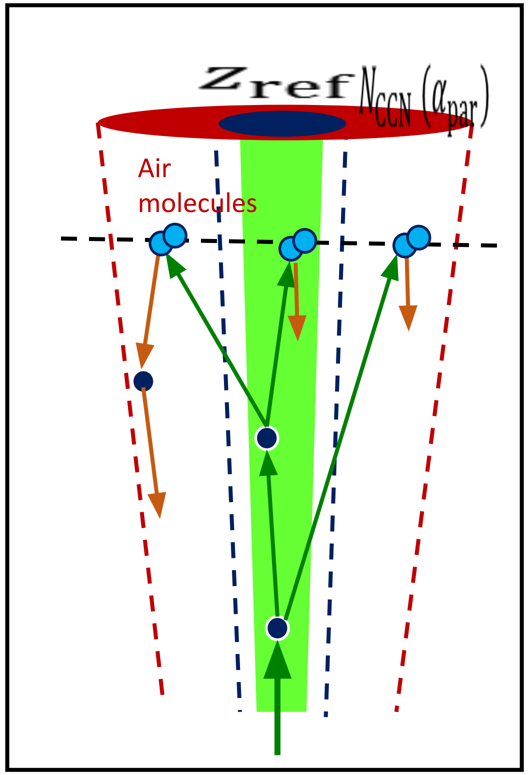

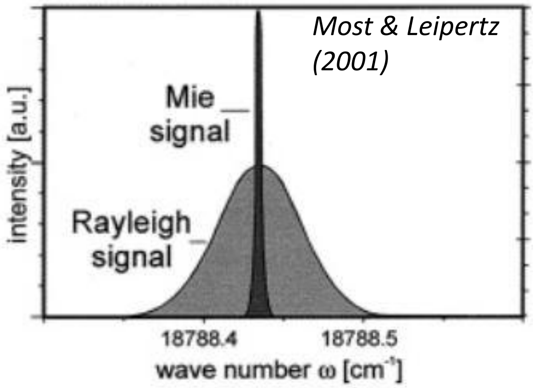

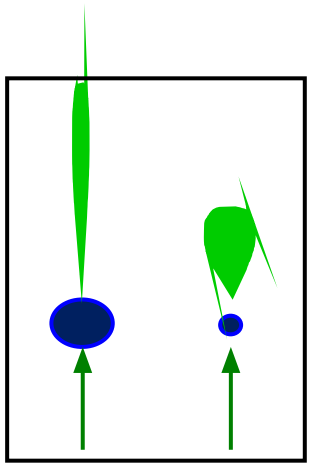

Phase function

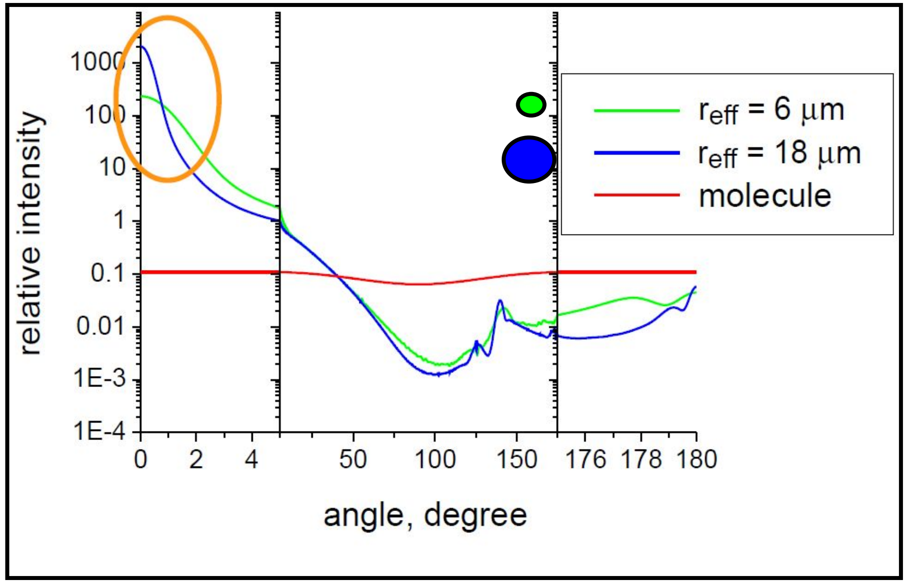

- **Pros:**
  - **Fast multiple-scattering model *(Malinka and Zege, 2003)*. No assumptions about the vertical structure.**
  - **No need of large averaging periods and can potentially works during daytime.**
- **Cons:**
  - **HSRL is technically challenging.**
  - **Expertise on the topic not so spread over the community.**

3. Dual-FOV polarization lidar

Jimenez et al., ACP 2020a, 2020b (since 2017)

Cloud at 3 km height, $z_{ref} = 75$ meters above cloud base

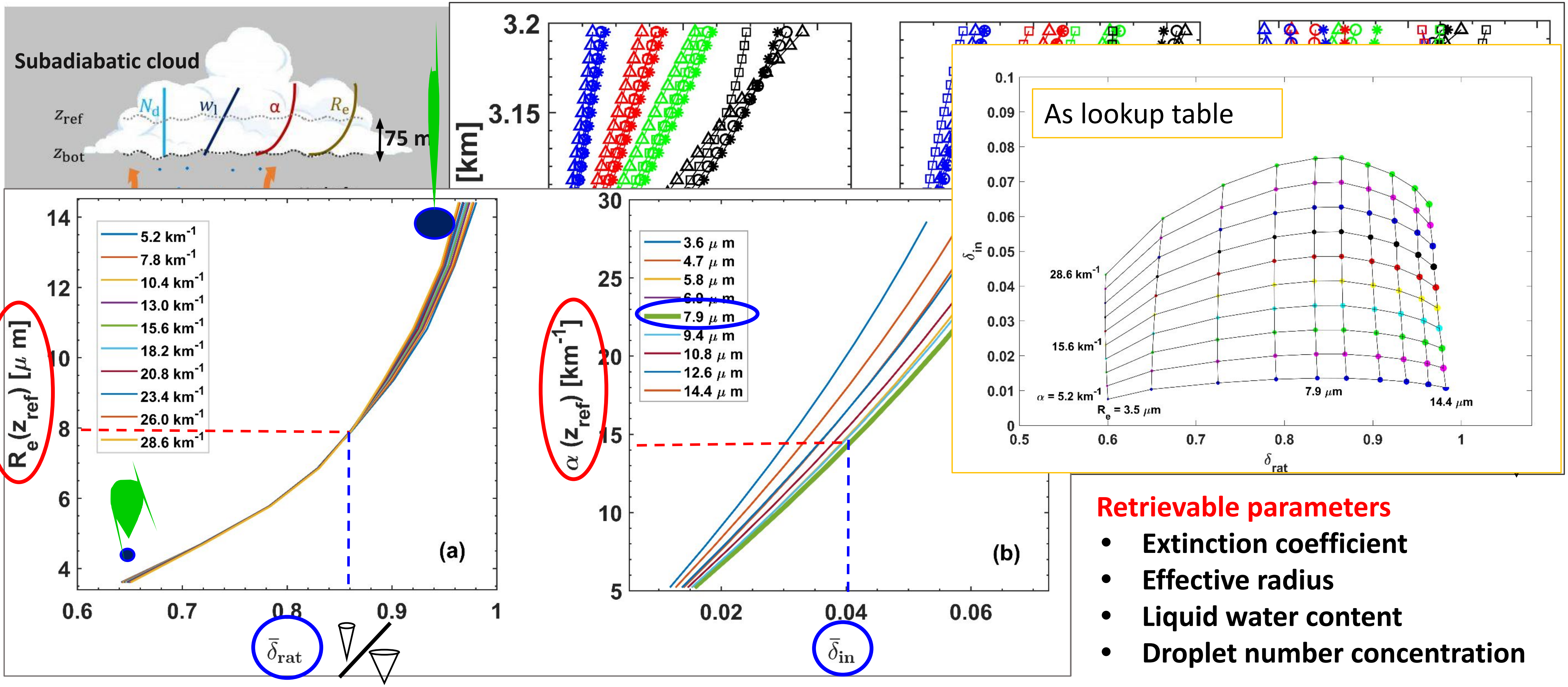

Retrievable parameters

- **Extinction coefficient**
- **Effective radius**
- **Liquid water content**
- **Droplet number concentration**

Instrumental upgrade and evaluation with measurements

MARTHA
(as Testbed)

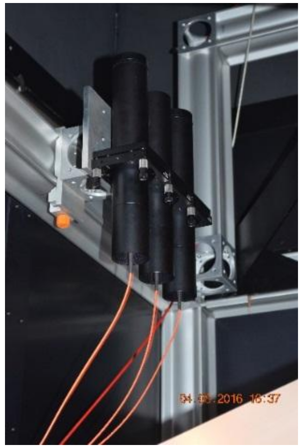

Polly XT
(as Workhorse)

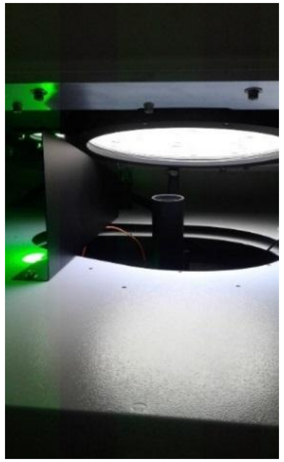

Calibration:
MARTHA: Three-signal approach (Jimenez et al., amt 2019)
Polly: Δ90 *degree approach (Engelmann et al., 2016, Freudenthaler, 2016)*

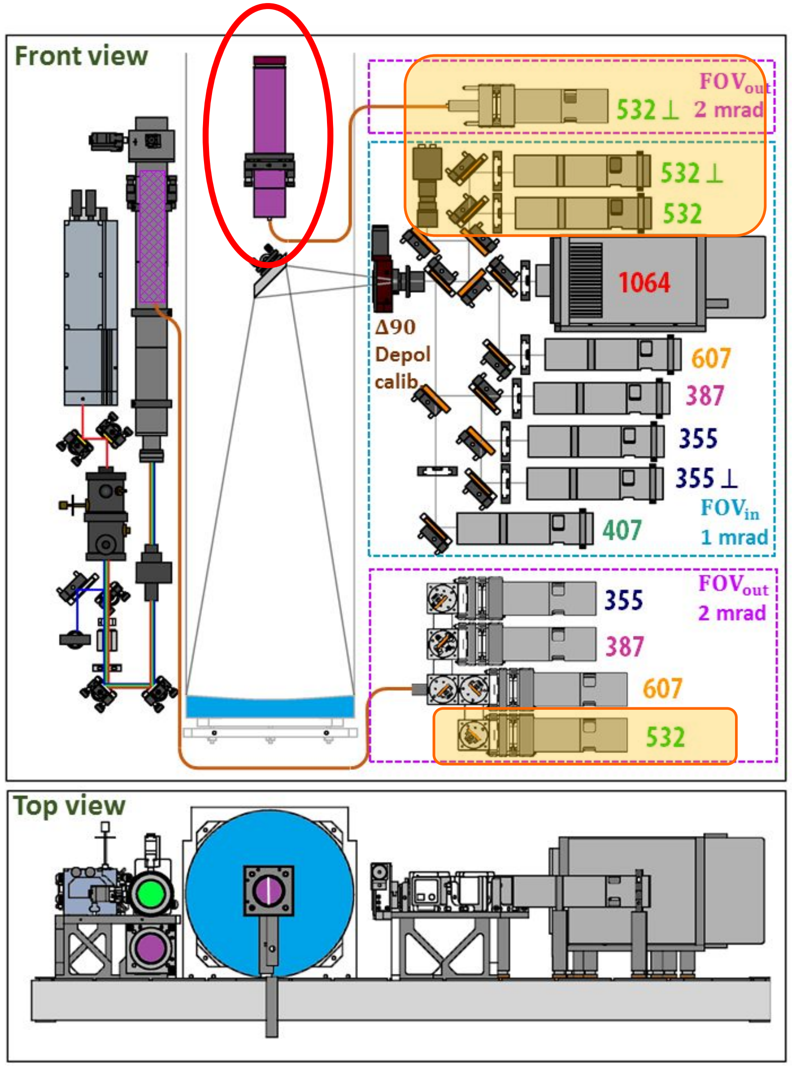

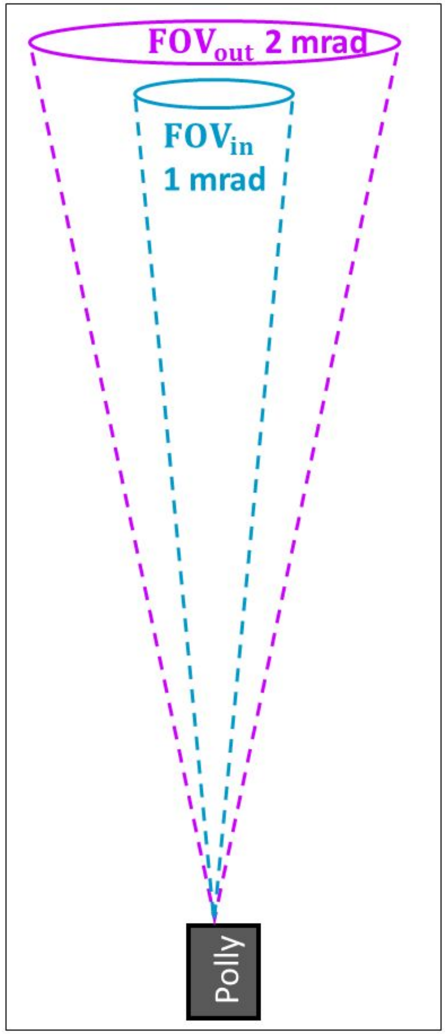

A measurement example

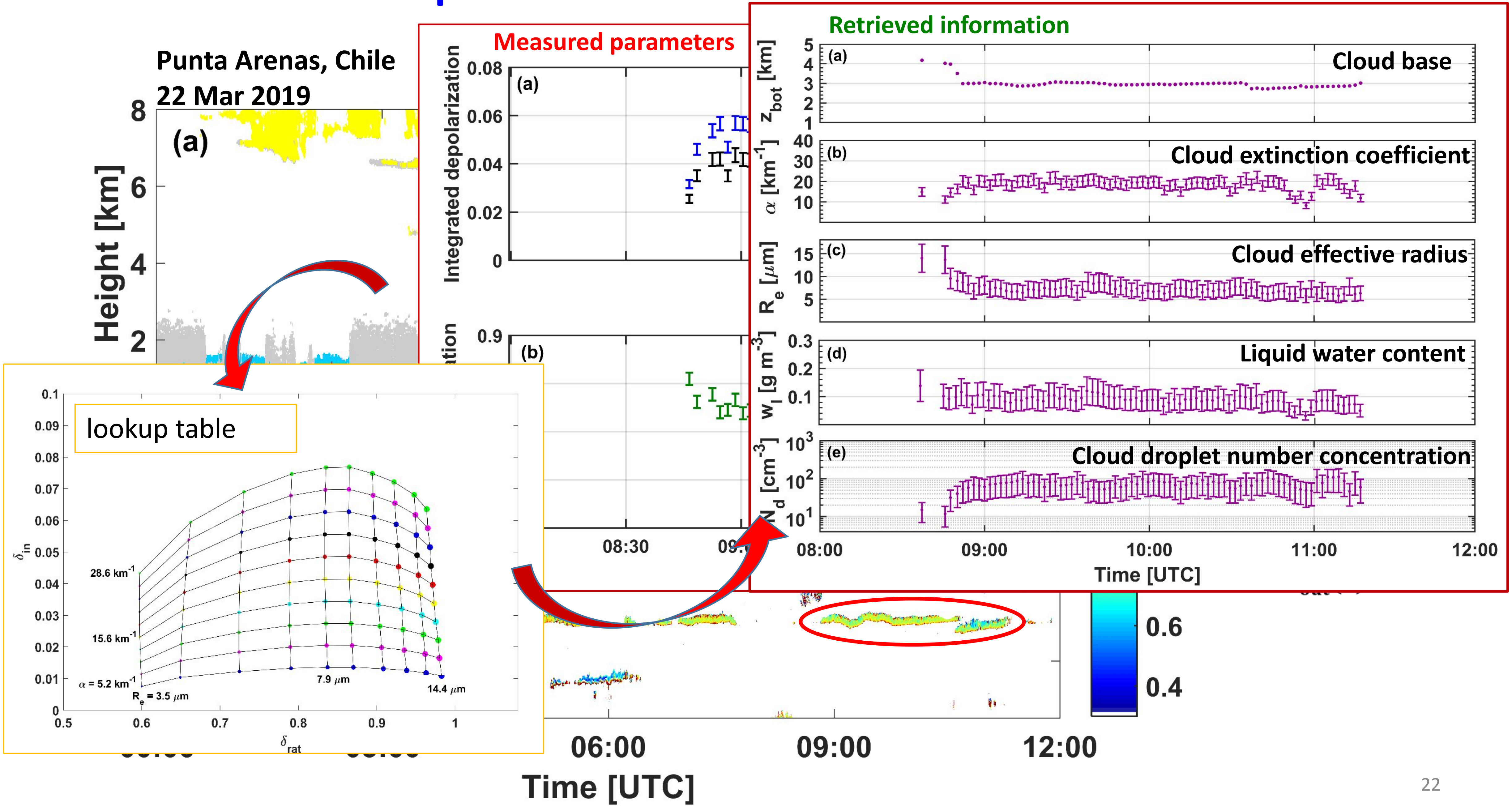

Aerosol cloud microphysical research capabilities at TROPOS

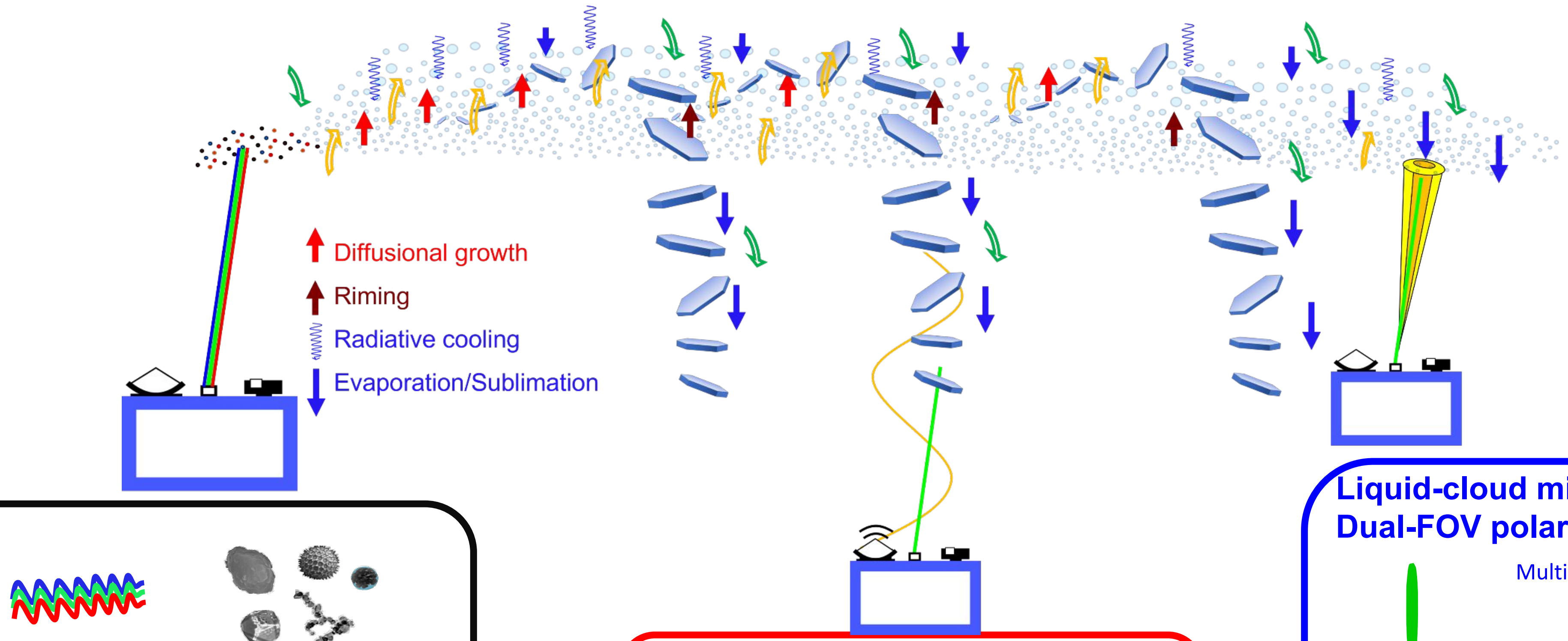

Aerosol microphysics – Multi-wavelength Raman polarization lidar

Aerosol type and extinction coefficient as input to derive number concentrations

$E \rightarrow N_{50}, N_{100}, N_{250}, S_{dry}$ $(\gamma_x E^{\sigma_x})$

+ Field and laboratory based parameterizations. CCN and INP concentrations

$\rightarrow CCNC, INPC_{i,d}$

(Mamouri and Ansmann, ACP, 2015, 2016. Ansmann et al., ACP, 2019, 2021)

Ice-cloud microphysics – Lidar-radar synergy

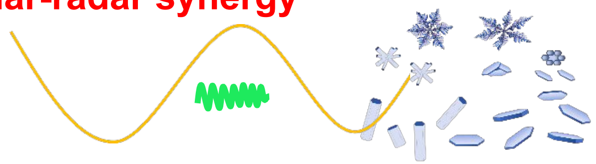

$$\frac{Z_{radar}}{E_{lidar}} \propto \frac{\int m^2(D)N(D)dD}{\int A((D))N(D)dD} \rightarrow D_0 \text{ (size)} \rightarrow ICN \text{ (Number)}$$

$m(D) = \gamma_m D^{\sigma_m}$, $A(D) = \gamma_A D^{\sigma_A}$

$N(D) = N_0 D^{\mu} \exp[-(3.67+\mu)D/D_0]$

$\gamma_m, \sigma_m, \gamma_A, \sigma_A$: Crystal shape dependent parameters. μ: width of size distribution, and D_0 the volumetric mean diameter.

(Bühl et al., AMT 2019, Mason et al., JGR, 2018)

Liquid-cloud microphysics – Dual-FOV polarization lidar

Multiple-scattering-based method

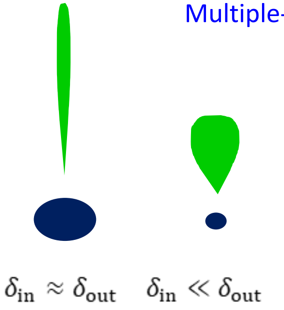

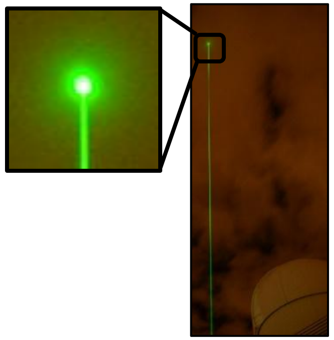

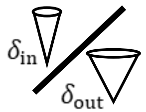

$R_e = \mathcal{P}_3(\frac{\delta_{in}}{\delta_{out}}, CB)$

$E = \mathcal{P}_2(\delta_{in}, CB, R_e)$

$\rightarrow R_e$ (size) $\rightarrow CD.$ (Number)

$$CDNC = \frac{1}{2\pi k} E R_e^{-2}$$

(Jimenez et al., ACP, 2020a,b, Jimenez 2021)

Long-term results of aerosol and clouds: Pristine vs Polluted

Punta Arenas, Chile
53.1° S, 70.9° W
Nov 2018 – Nov 2021

Dushanbe, Tajikistan
38.5° N, 68.8° E
June 2019 – present

Where are we with DFOV-polarization lidar

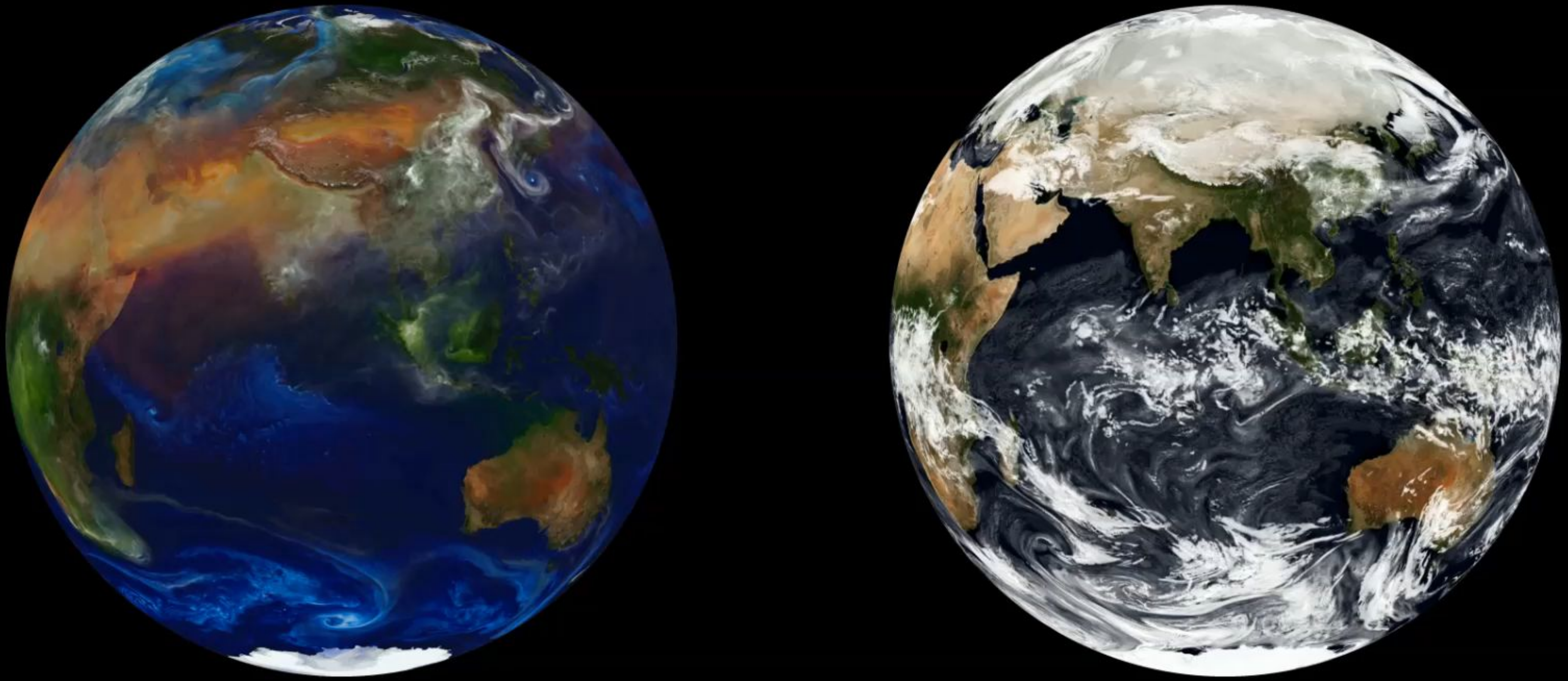

Adapted from NASA GEOS-5 Nature Run collection

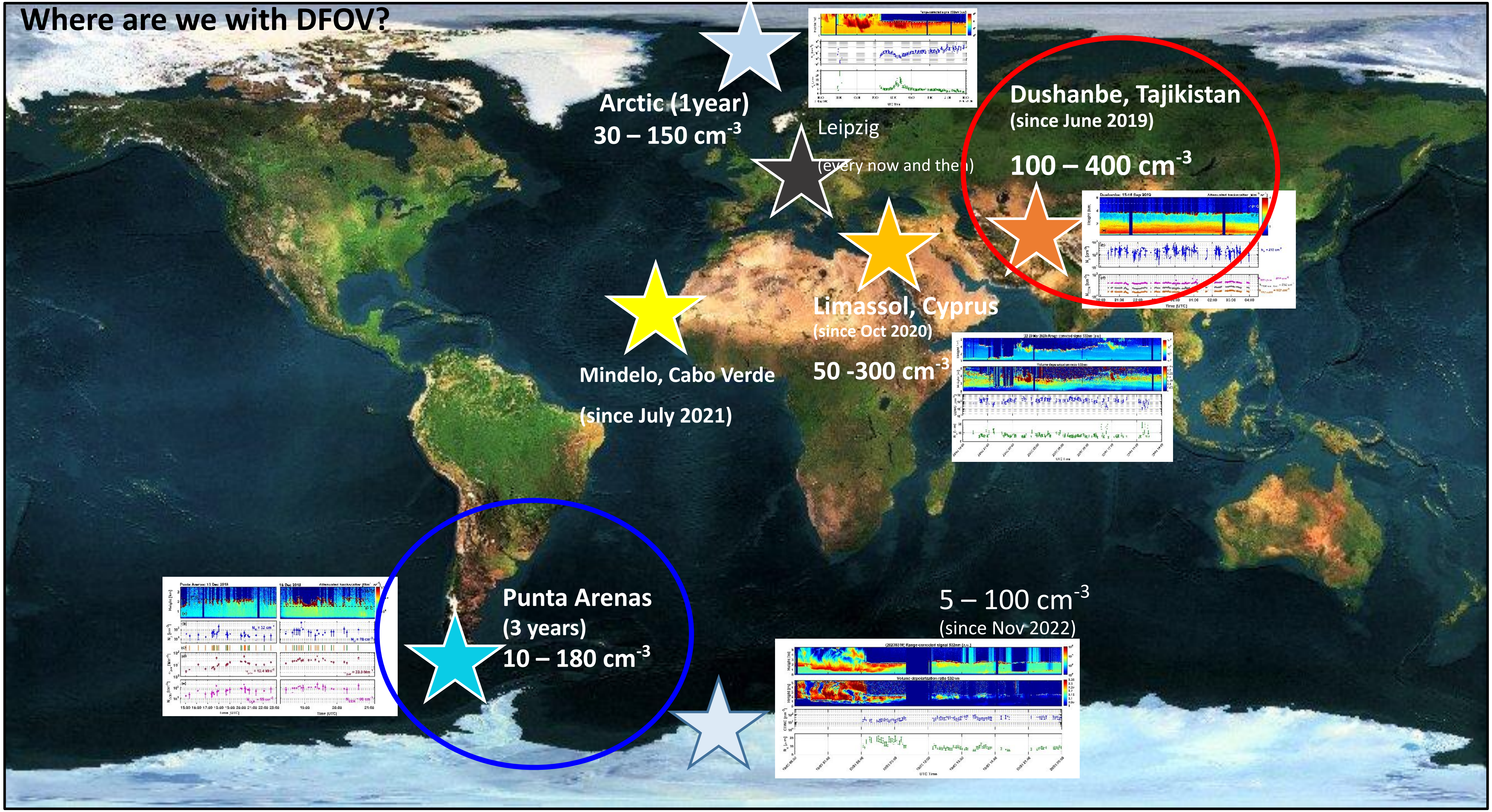
Where are we with DFOV?
Arctic (1year)
30 – 150 cm-3
Leipzig
(every now and then)
Dushanbe, Tajikistan
(since June 2019)
100 – 400 cm-3
Limassol, Cyprus
(since Oct 2020)
50 -300 cm-3
Mindelo, Cabo Verde
(since July 2021)
Punta Arenas
(3 years)
10 – 180 cm-3
5 – 100 cm-3
(since Nov 2022)

Lidar plots "polluted" vs. "clean"

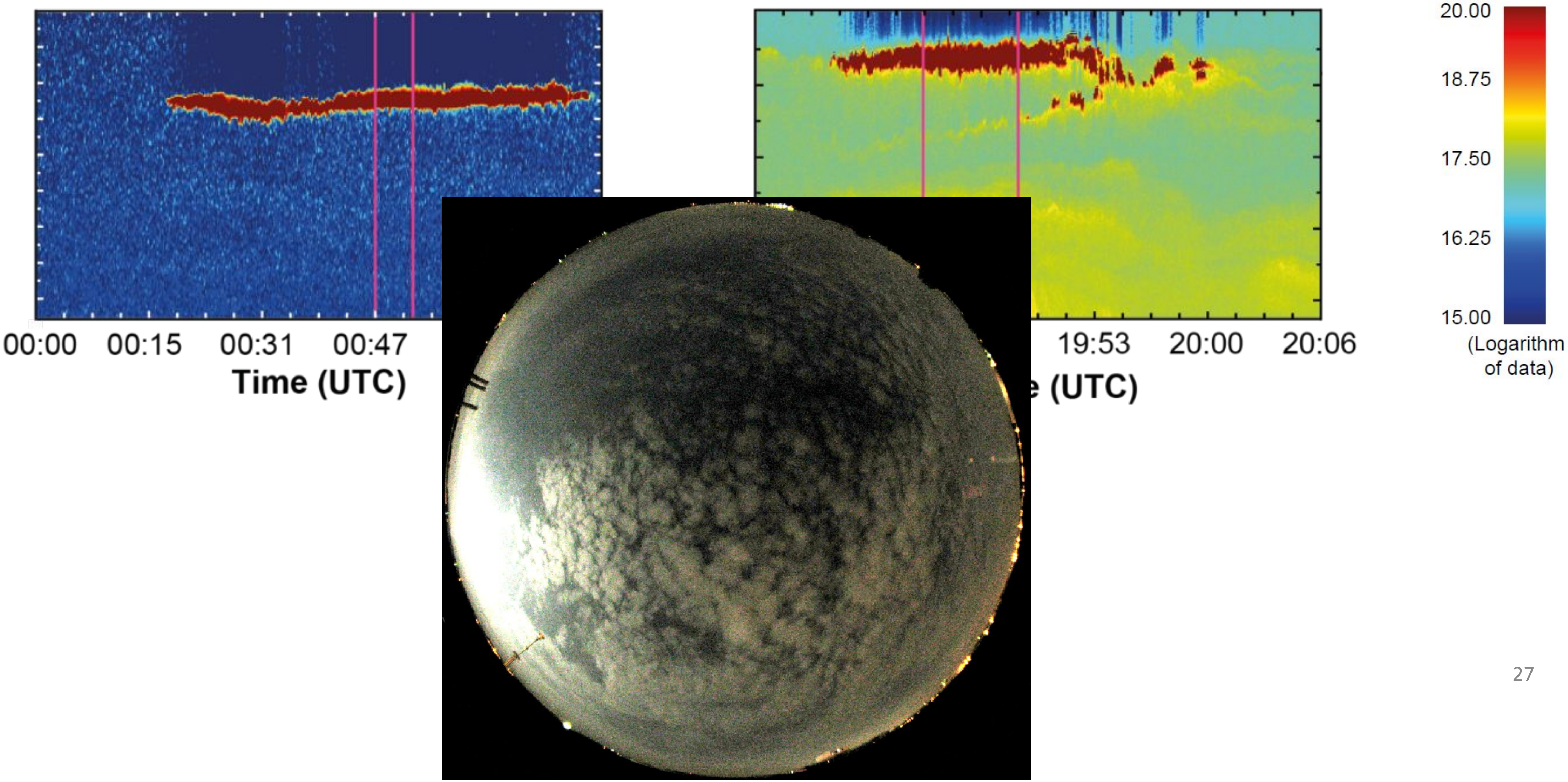

Long-term results of aerosol and clouds: Pristine vs Polluted

Cloud properties (75m above CB)

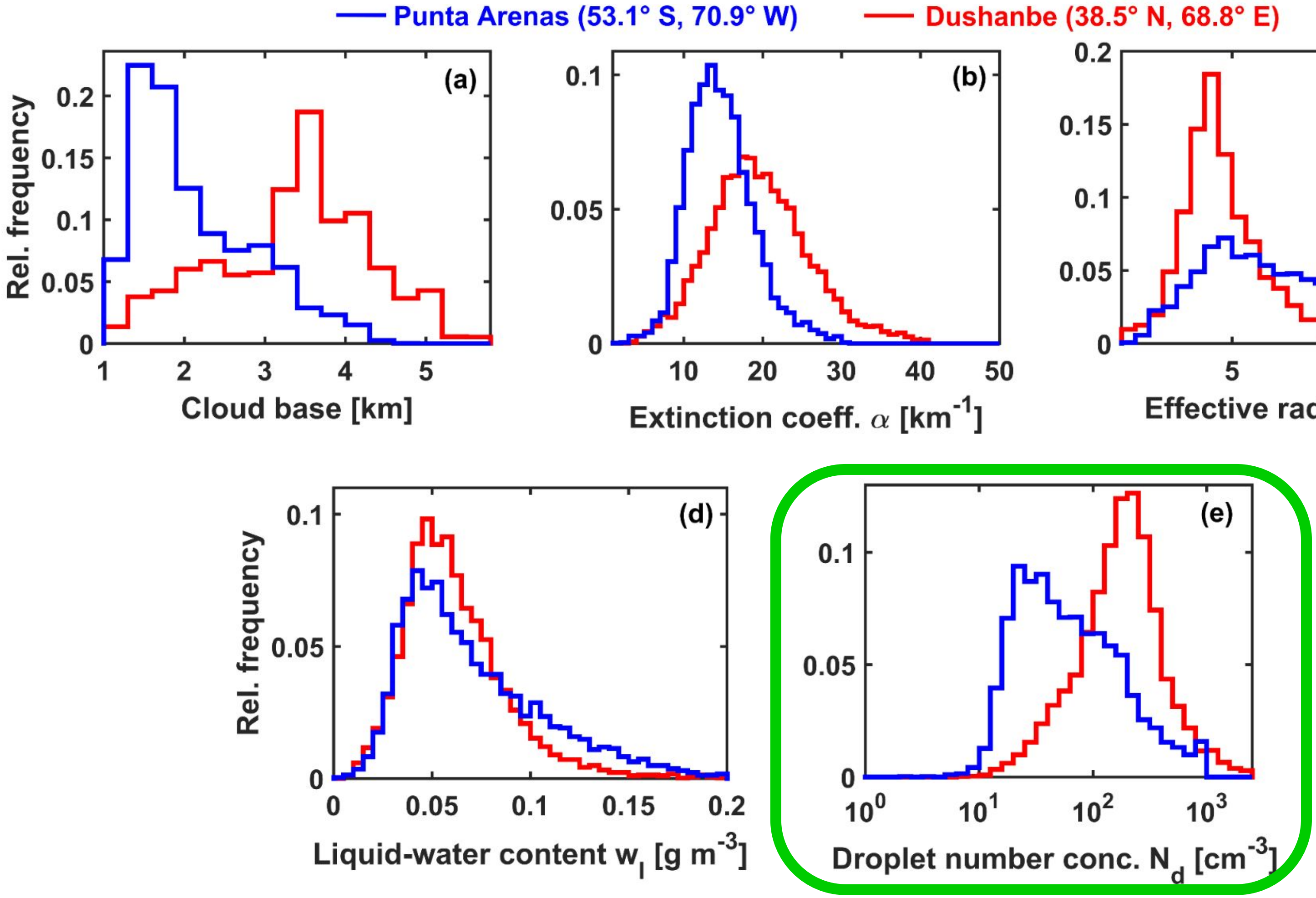

Punta Arenas

$$N_{CCN(0.2\%\ ss)} \approx N_d$$

Dushanbe

$$N_{CCN(0.2\%\ ss)} > 2\ N_d$$

Aerosol-cloud-interaction index (monthly basis)

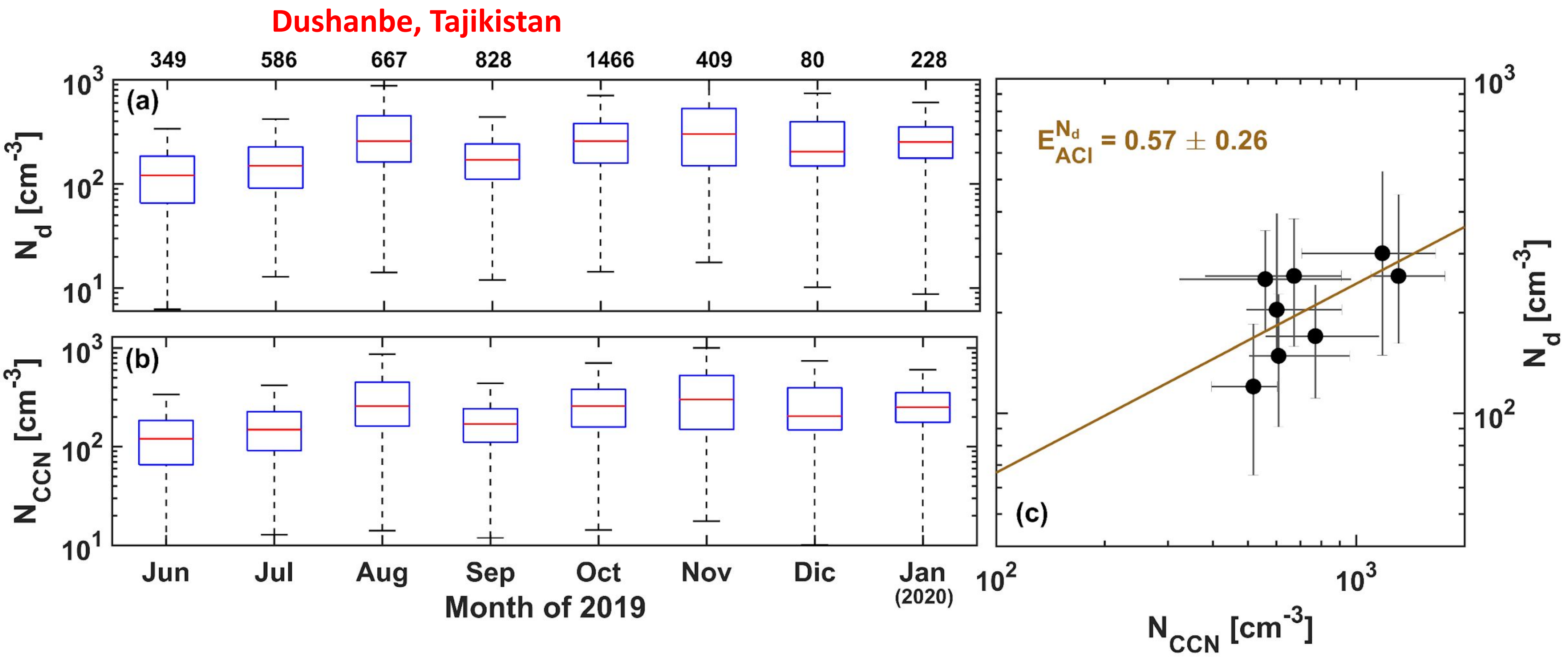

Relevance of these results for the radiative effect

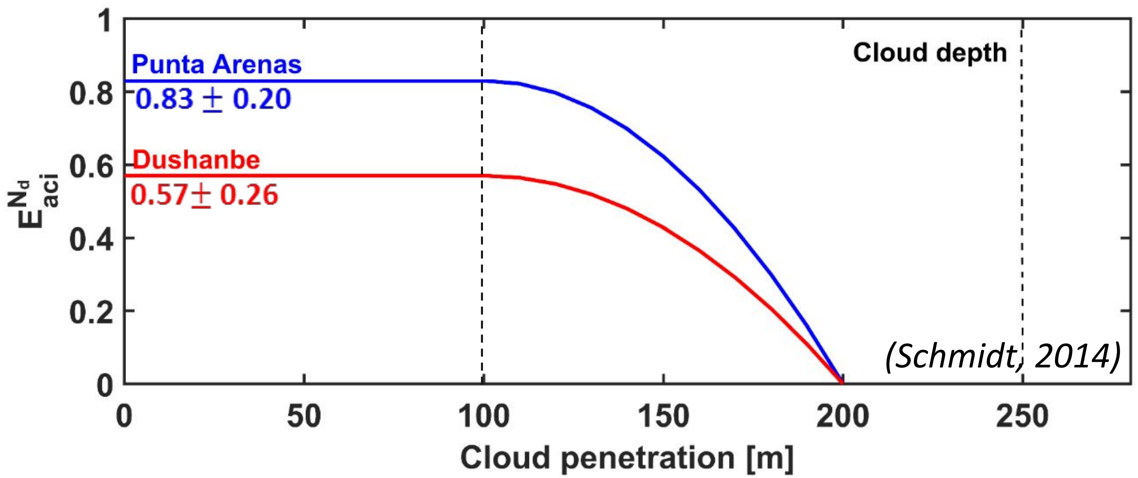

$$E_{\rm aci}^{\rm N_d,Twomey} \approx \frac{2}{3} E_{\rm aci}^{N_d}$$ → Obtained during this work

$$F_{\rm aci}^{\rm Twomey} = -\frac{1}{3} f_{\rm c} A_{\rm c}(1 - A_{\rm c}) E_{\rm aci}^{\rm N_d,Twomey} F^{\downarrow} \Delta \ln N_{\rm CCN}$$

(Ackerman et al., 2000)

Obtained from MERRA-2

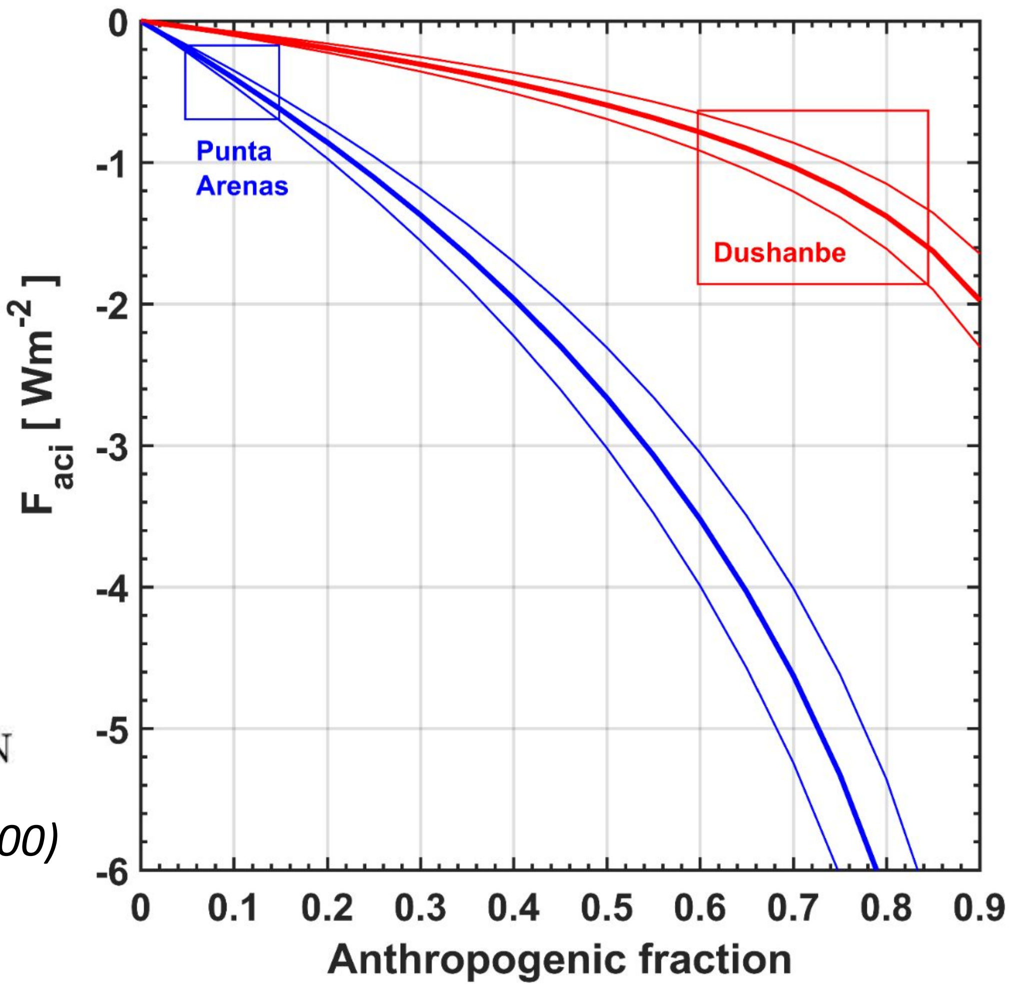

(Jimenez, 2021)

Lifecycle of mixed-phase clouds

Arctic-winter case

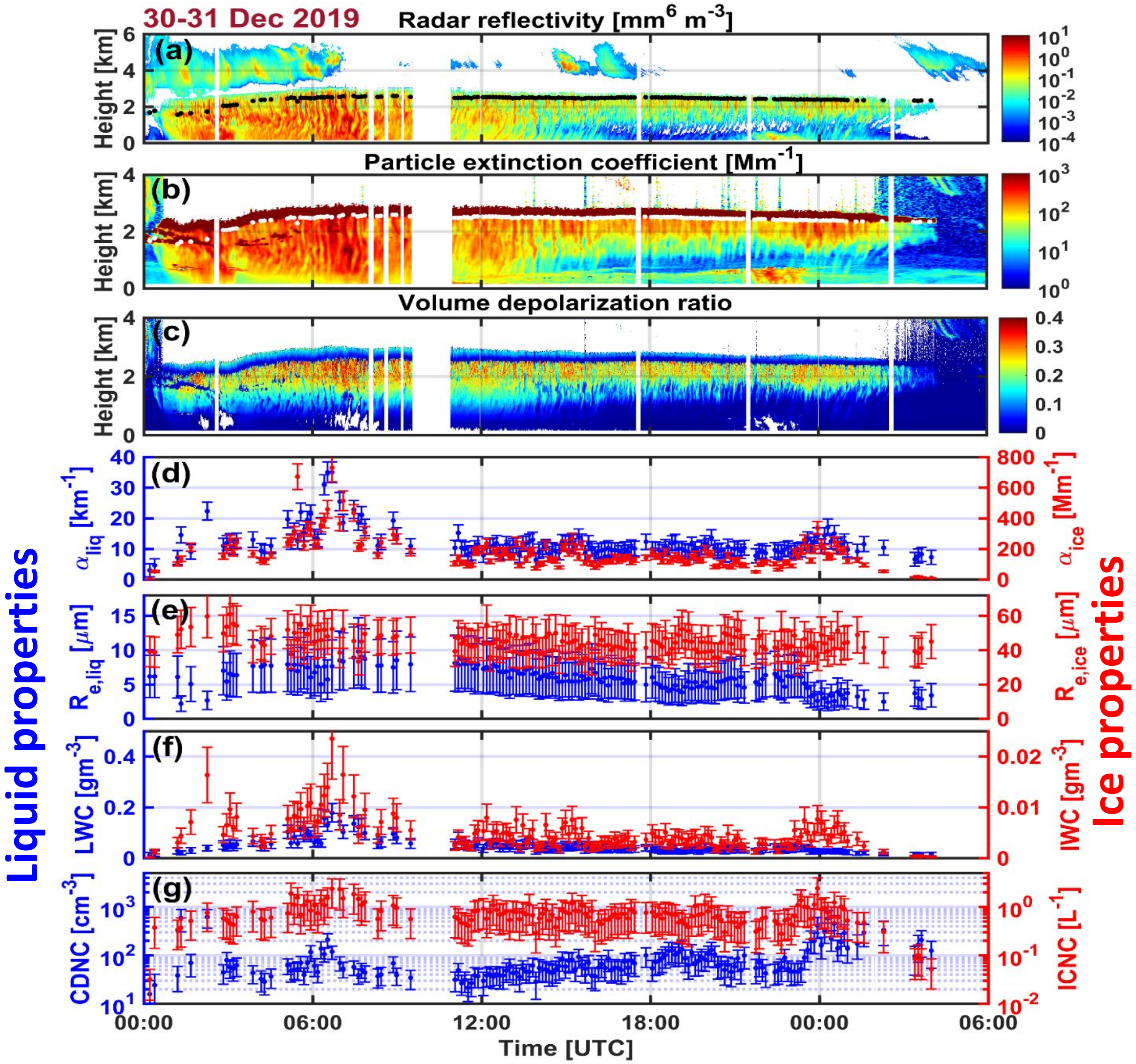

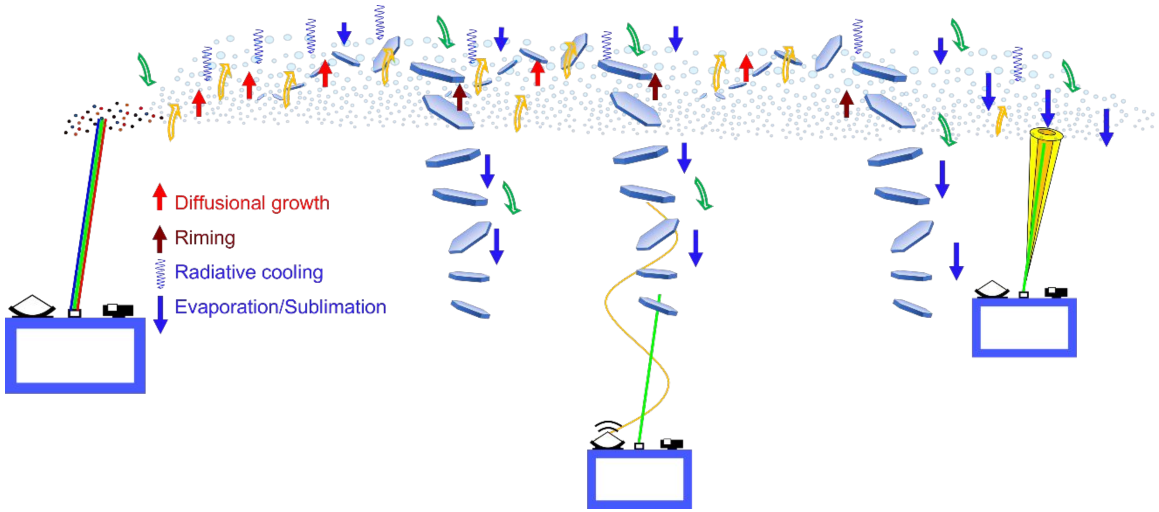

- Feeder-seeder and multilayering at the initial phase.
- Liquid and ice phases strongly correlated.
- MPS dominated by strong cloud-top cooling and large-scale lofting.
  Continuous activation of new droplets keep the cloud system alive.

(Jimenez et al., 2025, in preparation)

Lifecycle of mixed-phase clouds

Arctic-summer case

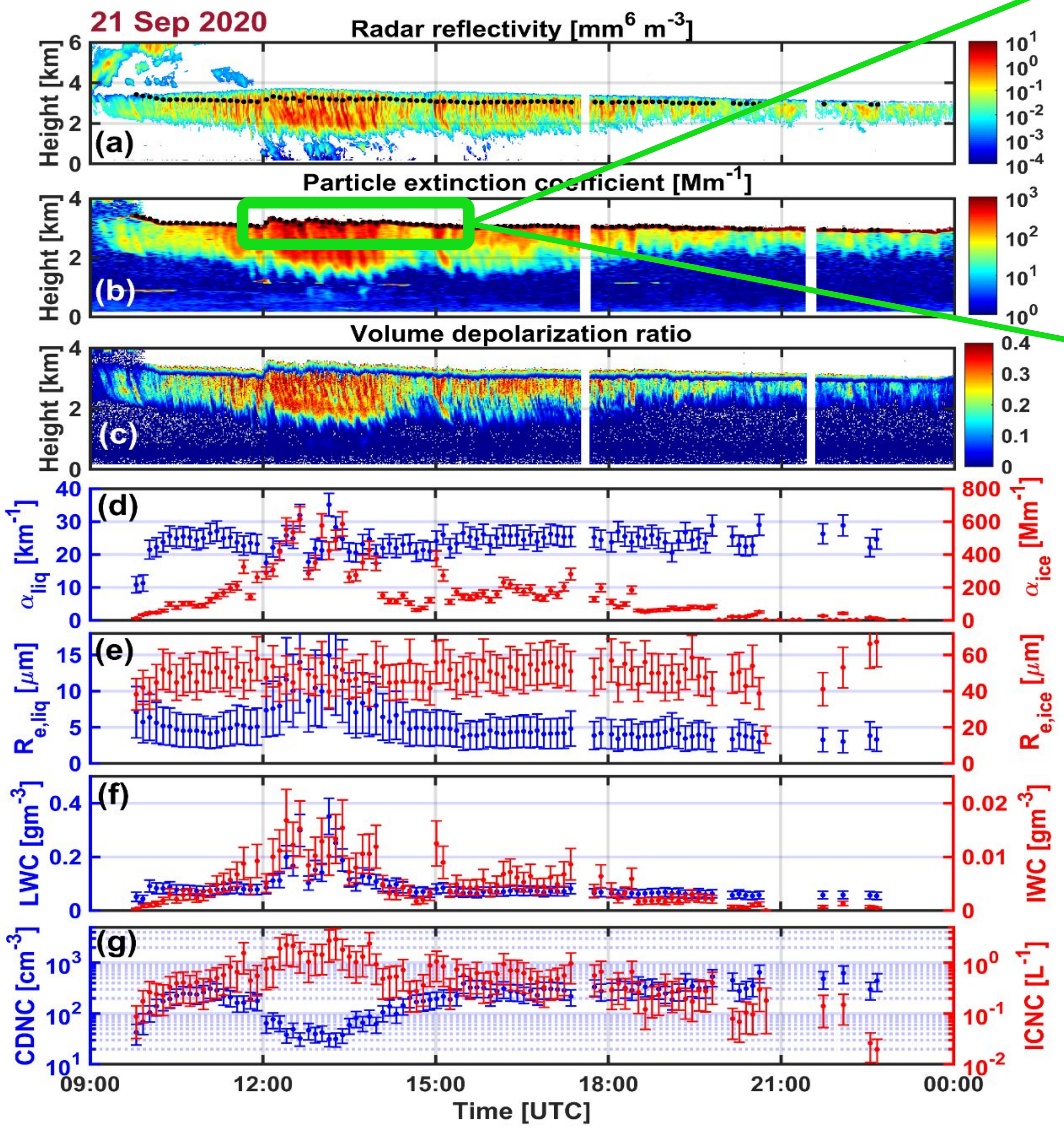

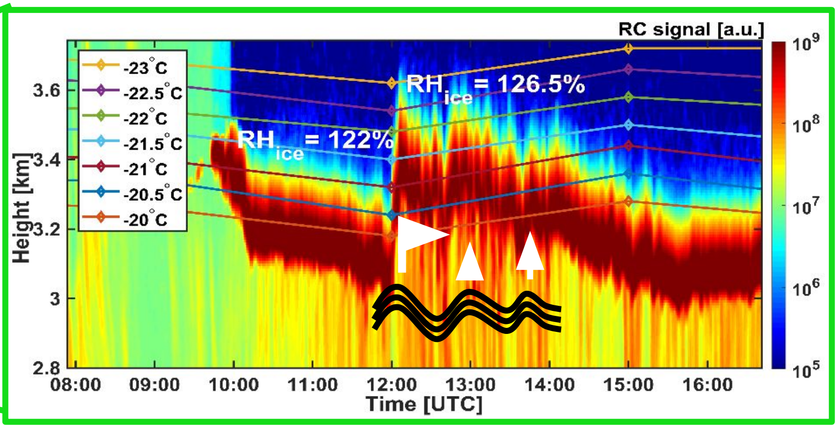

- More CCN and INP as well as water vapor available
- Liquid and ice phases
- External forcing alter the liquid-ice balance (likely from a gravity wave)
- Ice phase dominated during perturbation. Liquid phase recovered and dominated evolution in the next hours until cloud system vanishes as water vapor is consumed.

(Jimenez et al., 2025, ACP, accepted)

Summary

- Aerosol and clouds are key aspects for weather and climate research
- TROPOS is deeply involved in the developments of instruments and methods to characterize aerosol and clouds.
- Lidar multiple scattering is and issue but also an advantage in liquid water clouds.
- Several methods have been introduced to assess cloud microphysics using the multiple scattering effect:
  - Dual-FOV Raman (only nighttime, no high resolution)
  - Dual-FOV HSRL (daytime and high resolution, instrumentally challenging)
  - Dual-FOV polarization (daytime and high resolution, cloud assumed subadiabatic)
- Combined cloud and aerosol information can help to address aerosol-cloud interactions and study cloud processes.
  - 1st order aerosol-cloud interaction (Twomey effect)
  - In-cloud interplay between liquid and ice phases.

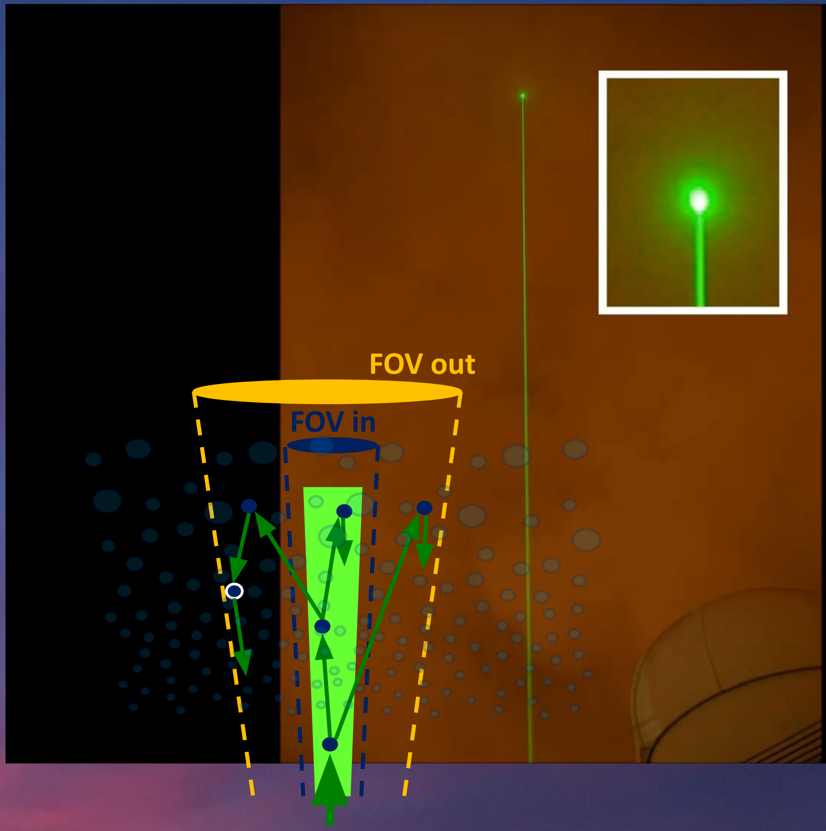

Thank you